

# EUROPEAN ORGANIZATION FOR NUCLEAR RESEARCH

ALEPH 2000-074 CONF 2000-051  
DELPHI 2000-148 CONF 447  
L3 Note 2600  
OPAL Technical Note TN661  
24 July, 2000  
Updated 28 July, 2000

## Searches for Higgs bosons: Preliminary combined results using LEP data collected at energies up to 209 GeV

ALEPH, DELPHI, L3 and OPAL Collaborations

The LEP working group for Higgs boson searches<sup>1</sup>

### Abstract

In the year 2000 the four LEP experiments have collected data at energies between 200 and 209 GeV, for approximately  $350 \text{ pb}^{-1}$  integrated luminosity with about  $120 \text{ pb}^{-1}$  above 206 GeV. The LEP working group for Higgs boson searches has combined these data with data sets collected earlier at lower energies. No statistically significant excess has been observed when compared to the Standard Model background prediction. The following 95% confidence level bounds have been obtained. For the Standard Model Higgs boson, the lower bound on the mass is  $113.3 \text{ GeV}/c^2$ . In the Minimal Supersymmetric Standard Model and from representative scans of the SUSY parameters, the mass limits  $m_h > 90.5 \text{ GeV}/c^2$  and  $m_A > 90.5 \text{ GeV}/c^2$  are obtained for the light CP-even and the CP-odd neutral Higgs boson, respectively. Furthermore, for a top quark mass less than or equal to  $174.3 \text{ GeV}/c^2$ , and assuming no (or large) mixing in the scalar-top sector, the range  $0.9 < \tan \beta < 7.7$  ( $0.5 < \tan \beta < 2.3$ ) is excluded. For charged Higgs bosons predicted by two-doublet extensions of the Standard Model and decaying only into the channels  $H^+ \rightarrow c\bar{s}$  and  $\tau^+ \nu$ , a lower bound of  $77.4 \text{ GeV}/c^2$  is obtained for the mass. In a “fermiophobic” two-doublet scenario where the decay  $H \rightarrow \gamma\gamma$  is expected to be enhanced, a lower mass bound of  $106.4 \text{ GeV}/c^2$  is obtained. Finally, if the neutral CP-even Higgs boson decays into “invisible” particles such as neutralinos, the lower bound on the mass is  $107.6 \text{ GeV}/c^2$ .

ALL RESULTS QUOTED IN THIS NOTE ARE PRELIMINARY  
Submitted to ICHEP'2000, Osaka, Japan, July 27 - August 2, 2000

---

<sup>1</sup>Contributions from S. Andringa, P. Bock, M. Carena, P. Colas, M. Felcini, I. Fisk, T. Fragat, P. Garcia-Abia, S. Heinemeyer, K. Hoffman, A. Holzner, D. Horváth, P. Igo-Kemenes, P. Janot, T. Junk, M. Kado, E. Lucci, P. Lutz, J. Marco, C. Martinez-Rivero, P. McNamara, W. Murray, K. Nagai, I. Nakamura, A.N. Okpara, M. Oreglia, A. Quadt, A. Raspereza; A. Read, A. Rosca, V. Ruhmann-Kleider, A. Sopczak, M. Stanitzki, P. Teixeira-Dias, A. Tilquin, C. Tully, C. Wagner, G. Weiglein, S. Yamashita.

# 1 Introduction

We present combined results from the ALEPH, DELPHI, L3 and OPAL Collaborations on searches for the Standard Model (SM) Higgs boson, for the neutral Higgs bosons  $h^0$  and  $A^0$  of the Minimal Supersymmetric Standard Model (MSSM), and for charged Higgs bosons predicted by extensions of the SM with two Higgs field doublets (2HD models), “fermiophobic” Higgs bosons decaying into a pair of photons, and neutral Higgs bosons decaying into “invisible” particles such as neutralinos. The results are obtained by combining the data collected in the year 2000 at centre-of-mass energies between 202 and 209 GeV with earlier data collected at lower energies [1]. The new data represent an integrated luminosity of approximately  $350 \text{ pb}^{-1}$  in total, with about  $120 \text{ pb}^{-1}$  above 206 GeV.

Unless explicitly specified, all cross-sections, branching ratios and many other physics quantities used in this combination of data are calculated within the HZHA program package, Version 3 [2].

Each experiment has generated Monte Carlo event samples for the Higgs signal and the various background processes, typically, at 202, 204, 206, 208 and 210 GeV energies. Cross-sections, branching ratios, distributions of the reconstructed mass and other discriminating variables relevant to the combination have been interpolated to energies which correspond to the data sets. In this procedure special care has been taken to the regions of kinematic cutoff where the signal and background distributions vary rapidly. It has been established that the interpolation procedures do not add significantly to the final systematic errors.

The statistical procedure adopted for the combination of the data and the precise definitions of the confidence levels  $CL_b$ ,  $CL_{s+b}$ ,  $CL_s$  by which the search results are expressed, are stated in Appendix A. The main sources of systematic error affecting the signal and background rate predictions are included taking into account correlations between search channels, LEP energies and individual experiments. This is done using an extension of the method of Cousins and Highland [3] where the confidence levels are the averages of a large ensemble of Monte Carlo experiments, each one with a different choice of signal and background, varied within the errors.

For the interpretation of the results in the MSSM, the LEP-Higgs working group has adopted a set of theoretical “benchmarks” [4], which are based on up-to-date calculations of radiative corrections. The parameters of these benchmark scans are described in Appendix B.

## 2 Combined searches for the SM Higgs boson

At LEP the SM Higgs boson is expected to be produced mainly via the Higgs-strahlung process  $e^+e^- \rightarrow HZ$ , while contributions from the  $WW \rightarrow H$  fusion channel,  $e^+e^- \rightarrow H\nu_e\bar{\nu}_e$ , are typically below 10%. The searches performed by the four LEP collaborations encompass the usual  $HZ$  final state topologies, commonly called ‘four-jet’ ( $HZ \rightarrow b\bar{b}q\bar{q}$ ), ‘missing energy’ ( $b\bar{b}\nu\bar{\nu}$ ),

‘leptonic’ ( $b\bar{b}e^+e^-$  and  $b\bar{b}\mu^+\mu^-$ ), and ‘tau’ channels ( $b\bar{b}\tau^+\tau^-$  and  $\tau^+\tau^-q\bar{q}$ ). The searches in the missing energy channel are optimized for Higgs-strahlung, but are also sensitive to the  $WW \rightarrow H$  fusion process. From combining the earlier data collected by the LEP experiments at center of mass energies up to 202 GeV, a 95% CL lower bound of  $107.9 \text{ GeV}/c^2$  has been obtained [1]. In this section we present an update of the SM Higgs boson search which includes the new data collected in the year 2000 at centre-of-mass energies up to 209 GeV.

The analysis procedures of the four LEP experiments producing the inputs for the present combination are described in individual documents [5, 6, 7, 8, 9]; we merely summarise the results in Table 1. The large spread in the numbers of selected candidates reflects substantial differences in the selection methods and optimisation procedures. All events which make an entry to Table 1 are used below in the calculation of confidence levels and in the limit setting procedure.

The test-statistic (of Eq. 1 of Appendix A denoted here as  $Q$ ) versus the test mass  $m_H$ , computed for the observed results, is shown in Figure 1. It should have a minimum near the true Higgs mass. A negative value would indicate some preference for the signal hypothesis and the more negative the value the more significant the result. The full-line curve representing the observation is in good agreement with the dashed line representing the background hypothesis, and deviates from the dotted curves which represent signal + background situations with true Higgs boson masses fixed at particular values.

The compatibility with background of the result is given by  $1 - CL_b$ , which is plotted as a function of  $m_H$  in Figure 2. Values of  $1 - CL_b$  below  $5.7 \times 10^{-7}$ , indicated by the horizontal full line, corresponding to a 5 standard deviation fluctuation of the background, are considered in the discovery region. The dotted line shows the expectation in the presence of a signal of true mass  $m_H$ ; its crossing with the  $5\sigma$  line at  $109.5 \text{ GeV}/c^2$  indicates the range of sensitivity of the presently available data to a discovery.

However, it is not enough just to read off the value of  $1 - CL_b$  at the minimum of the  $-2\ln(Q)$  to claim a signal since this only gives the probability that the background fluctuated at precisely *that* mass, while in principle it could have fluctuated anywhere in the mass region inspected (which is not already excluded strongly by previous searches and up to the limit of sensitivity). An estimate based on Monte Carlo studies shows that  $1 - CL_b$  must be multiplied by a factor four in the present case, corresponding roughly to the width of the mass search region divided by the typical mass resolution.

A 95% confidence level lower limit on the Higgs mass may be set by identifying the mass region where  $CL_s < 0.05$ , as shown in Figure 3. The median limit expected in the absence of a signal is  $113.4 \text{ GeV}/c^2$  and the limit observed by combining the LEP data is  $113.3 \text{ GeV}/c^2$ . The inclusion of systematic errors, together with their correlations, has decreased the limits by less than  $100 \text{ MeV}/c^2$ .

## STANDARD MODEL HIGGS - PRELIMINARY

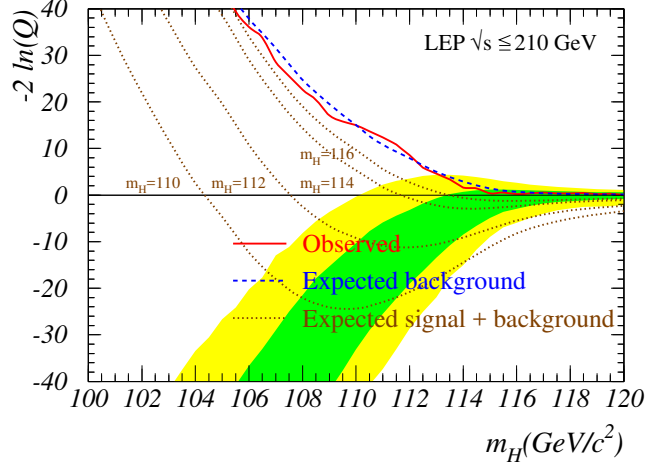


Figure 1: The negative log-likelihood ratio (test-statistic) as a function of  $m_H$ . The dashed line shows the expectation for the background-only hypothesis and the full line the values computed from the observed results. The shaded bands show the  $1\sigma$  and  $2\sigma$  probability bands for the signal at the “true” mass. The expected signal curves (dotted) show the median response away from the true mass for three different Higgs masses.

## STANDARD MODEL HIGGS - PRELIMINARY

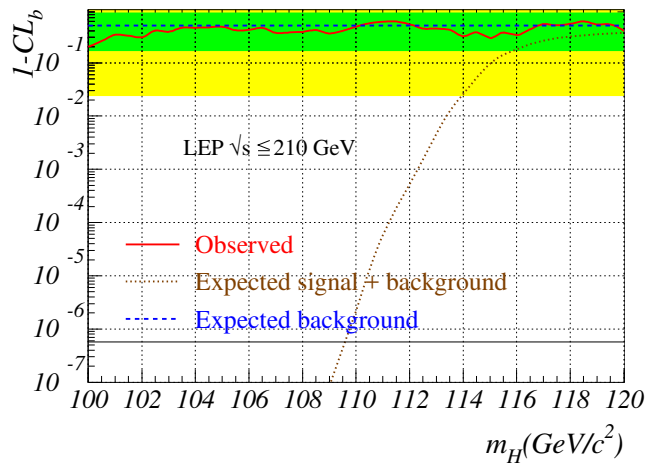


Figure 2: The confidence level  $CL_b$  as a function of  $m_H$ . The straight dashed line at 50% and the shaded bands represent the median result and the  $\pm 1\sigma$  and  $\pm 2\sigma$  probability bands expected in the absence of a signal. The solid curve is the observed result and the dotted curve shows the median result expected for a signal when tested at the “true” mass. The horizontal line at  $5.7 \times 10^{-7}$  indicates the level for a 5 $\sigma$  discovery.

| Experiment:   | ALEPH     | DELPHI      | L3          | OPAL      |
|---|-----------|-------------|-------------|-----------|
| < 204.5 GeV: Integrated luminosity (pb <sup>-1</sup> ):     | 10.6      | 9.0         | 9.4         | 9.5       |
| Backg. predicted / Evts. observed                           | 6.4 / 8   | 12.4 / 9    | 2.0 / 2     | 3.2/1     |
| Four-jet:   | 2.2 / 4   | 7.1 / 4     | 1.3 / 1     | 1.1/1     |
| Missing-energy:   | 2.2 / 3   | 4.1 / 4     | 0.53 / 1    | 1.6/0     |
| Leptonic (e, $\mu$ ):                                       | 1.4 / 1   | 0.9 / 0     | 0.084 / 0   | 0.36/0    |
| Tau channels:   | 0.6 / 0   | 0.3 / 1     | 0.061 / 0   | 0.15/0    |
| 204.5-205.5 GeV: Integrated luminosity (pb <sup>-1</sup> ): | 52.5      | 53.4        | 45.4 - 46.5 | 44.0      |
| Backg. predicted / Evts. observed                           | 31.4 / 26 | 73.6 / 81   | 12.0 / 8    | 14.8/18   |
| Four-jet:   | 11.2 / 7  | 42.0 / 53   | 8.2 / 4     | 4.9/6     |
| Missing-energy:   | 9.7 / 10  | 24.5 / 23   | 2.9 / 2     | 7.5/5     |
| Leptonic (e, $\mu$ ):                                       | 7.2 / 5   | 5.3 / 4     | 0.47 / 1    | 1.7/7     |
| Tau channels:   | 3.3 / 4   | 1.8 / 1     | 0.36 / 1    | 0.72/0    |
| >205.5 GeV: Integrated luminosity (pb <sup>-1</sup> ):      | 31.1      | 33.7        | 27.0 - 28.8 | 26.5      |
| Backg. predicted / Evts. observed                           | 18.2 / 19 | 45.9 / 44   | 8.1 / 8     | 8.9/2     |
| Four-jet:   | 6.8 / 7   | 27.3 / 30   | 5.5 / 6     | 3.0/0     |
| Missing-energy:   | 5.1 / 6   | 14.2 / 12   | 1.9 / 2     | 4.5/1     |
| Leptonic (e, $\mu$ ):                                       | 4.3 / 3   | 3.3 / 1     | 0.47 / 0    | 1.0/1     |
| Tau channels:   | 2.0 / 3   | 1.1 / 1     | 0.26 / 0    | 0.43/0    |
| Total: Integrated luminosity (pb <sup>-1</sup> ):           | 94.2      | 96.1        | 81.8 - 84.7 | 80.0      |
| Backg. predicted / Evts. observed                           | 56.1 / 53 | 131.9 / 134 | 22.1 / 18   | 26.8 / 21 |
| Four-jet:   | 20.2 / 18 | 76.4 / 87   | 15.0 / 11   | 8.9 / 7   |
| Missing-energy:   | 17.0 / 19 | 42.8 / 39   | 5.3 / 5     | 13.6 / 6  |
| Leptonic (e, $\mu$ ):                                       | 12.9 / 9  | 9.5 / 5     | 1.0 / 1     | 3.0 / 8   |
| Tau channels:   | 5.9 / 7   | 3.2 / 3     | 0.69 / 1    | 1.3 / 0   |
| Events in all channels                                      | 56.1 / 53 | 131.9 / 134 | 22.1 / 18   | 26.8 / 21 |
| Limit (GeV/c <sup>2</sup> ) exp. (median) at 95% CL:        | 112.0(*)  | 109.2       | 108.0       | 109.5     |
| Limit (GeV/c <sup>2</sup> ) observed at 95% CL:             | 110.8(*)  | 109.0       | 107.7       | 109.5     |

Table 1: *Information related to the searches of the four LEP experiments for the SM Higgs boson at energies between 200 and 209 GeV (year 2000 data). In the L3 analysis the event selection, and thus the expected background and observed number of events, depend on the Higgs boson mass hypothesis; they are given here for  $m_H=110$  GeV/c<sup>2</sup>. (\*)In the ALEPH publication the confidence level estimator used is different from the one used by the other collaborations.*

## STANDARD MODEL HIGGS - PRELIMINARY

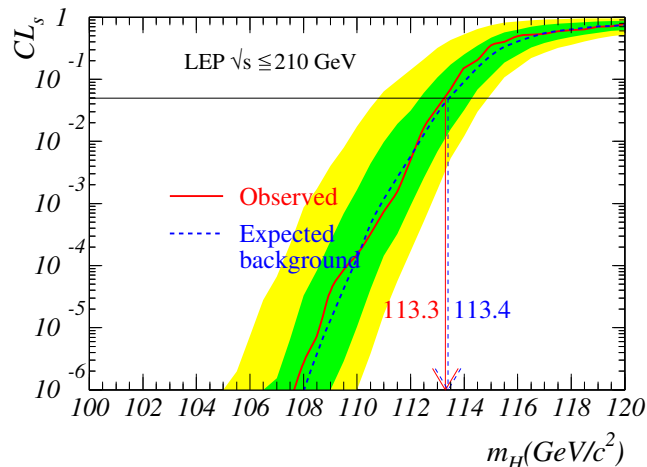


Figure 3: The confidence level  $CL_s$  for the signal hypothesis versus  $m_H$ . The solid curve is the observed result, the dashed curve the median result expected in the absence of a signal. The shaded areas represent the symmetric  $1\sigma$  and  $2\sigma$  probability bands of  $CL_s$  in the absence of a signal. The intersections of the curves with the horizontal line at  $CL_s = 0.05$  give the mass limits at the 95% confidence level.

As a cross-check of the confidence level calculation procedures, the expected and observed limits have been calculated independently, using another test-statistic (Method C in [10]). The observed and expected limits are within  $\pm 100$  MeV/ $c^2$  of the values quoted above.

Figure 4 shows the distribution of reconstructed Higgs masses for a subset of the events in Table 1. The corresponding background from SM processes and the signal expected from a SM Higgs boson of 110 GeV/ $c^2$  mass are also shown. The figure has been obtained with the supplementary requirement that the contributions from the four experiments (selecting the most signal-like set of events) be roughly equal. Since all events enter with equal weight, such a distribution does not reflect for example differences in mass resolutions, signal sensitivities and background rates, which characterise the various search channels and individual experiments.

## STANDARD MODEL HIGGS - PRELIMINARY

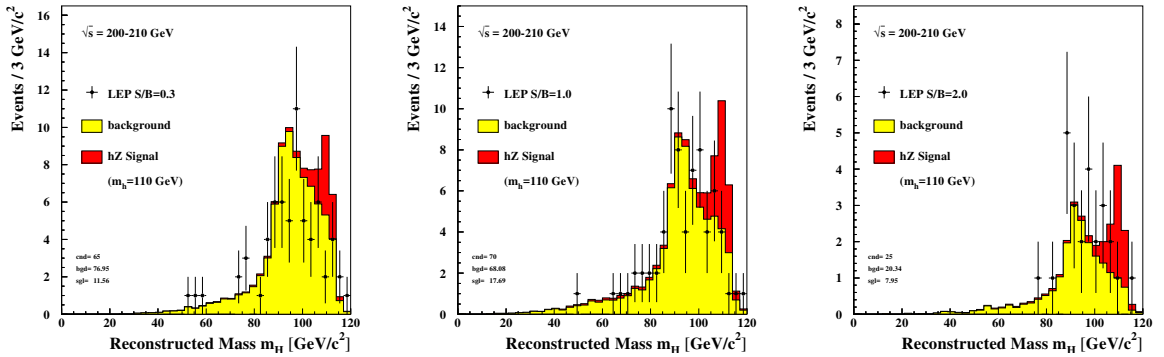


Figure 4: *Reconstructed mass of all candidates from the 4 LEP experiments satisfying (a)  $S/B > 0.3$ , (b)  $S/B > 1.0$ , (c)  $S/B > 2.0$ . The  $S/B$  cut applies to the region  $m > 105$  GeV/ $c^2$  and for  $m_h = 110$  GeV/ $c^2$ .*

### 3 Combined searches for the Higgs bosons $h$ and $A$ in the MSSM

In the MSSM there are two fundamental Higgs field doublets, and the Higgs sector comprises five physical states: two CP-even neutral Higgs bosons,  $h$  and  $H$  ( $m_h < m_H$ ), one CP-odd neutral Higgs boson,  $A$ , and a pair of charged Higgs bosons,  $H^+$  and  $H^-$ . At LEP energies the  $h$  and  $A$  particles are expected to be produced mainly via the Higgs-strahlung process  $e^+e^- \rightarrow hZ$  (analogous to the main MSM production process) or the pair production process  $e^+e^- \rightarrow hA$ . The two processes are complementary: the cross-section of the first is proportional to  $\sin^2(\beta - \alpha)$  and that of the second proportional to  $\cos^2(\beta - \alpha)$  ( $\tan \beta$  is the ratio of the vacuum expectation values of the two Higgs field doublets and  $\alpha$  is a mixing angle in the CP-even Higgs sector).

The combined data of the four LEP experiments are interpreted here within the framework of a ‘constrained’ MSSM where universal values  $M_{\text{SUSY}}$  and  $M_2$  are assumed for the SUSY breaking sfermion and gaugino masses, respectively, at the electroweak scale. Combined search results are given for three new ‘benchmark’ MSSM parameter scans [4], which are described in Appendix B. The first benchmark corresponds to *no-mixing* in the scalar-top sector; a second to large mixing and the parameters tuned to maximise the parameter space along  $m_h$  ( $m_h$ -*max* hereafter); a third scan (*large- $\mu$*  hereafter) is designed to highlight choices of MSSM parameters for which the  $h^0$  does not decay into  $b\bar{b}$  due to large loop corrections. In all three benchmark scans the top mass, which has a large impact on the results via radiative corrections, is fixed to the experimental central value of  $m_t = 174.3 \text{ GeV}/c^2$  [11], and to two alternative values where the central value is decreased and increased by the current experimental error of  $5.1 \text{ GeV}/c^2$ . In each case, the exclusion limits obtained are valid for  $m_t$  less than or equal to the chosen value, since the predicted value of  $m_h$  increases with  $m_t$ .

The individual searches of the four LEP collaborations for the processes  $e^+e^- \rightarrow hZ$  and  $e^+e^- \rightarrow hA$  which include the data taken at  $\sqrt{s}$  from 200 to 209 GeV (year 2000 data), are described in [5, 6, 7, 9, 12]. For the process  $e^+e^- \rightarrow hZ$ , the searches for the SM Higgs boson are interpreted in the MSSM while taking into account the reduced cross-section due to the factor  $\sin^2(\beta - \alpha)$  and the predicted variations of the decay branching ratios of the  $h$  boson in the scans. For the process  $e^+e^- \rightarrow hA$ , the most relevant final states are  $b\bar{b}b\bar{b}$ ,  $\tau^+\tau^-b\bar{b}$  and  $b\bar{b}\tau^+\tau^-$ . In the kinematic domain  $2m_A < m_h$ , besides decaying into the usual fermionic final states, the  $h$  boson can also decay via the process  $h \rightarrow AA$ . The collaborations have included the  $h \rightarrow AA$  decay in their searches either by applying the standard  $hZ$  and  $hA$  search procedures with efficiencies calculated for the  $(AA)Z$  and  $(AA)A$  final states or by performing specific searches for these final states.

The experimental results are also interpreted in terms of heavy Higgs boson production in the Higgsstrahlung process when it is favoured. The cross-section for the process  $e^+e^- \rightarrow HZ^0$  is proportional to  $\cos^2(\beta - \alpha)$  and may be larger than that for  $e^+e^- \rightarrow hZ^0$  when the  $H$  is kinematically accessible, which occurs in the *large- $\mu$*  scan. If  $\sigma(e^+e^- \rightarrow HZ) \times \text{Br}(H \rightarrow b\bar{b}) > \sigma(e^+e^- \rightarrow hZ) \times \text{Br}(h \rightarrow b\bar{b})$  then the searches are interpreted as searches for  $HZ^0$  production and not  $hZ^0$  production, using the appropriate cross-sections and branching ratios for the  $H$  instead

of those for the h. The cross-sections are compared at  $\sqrt{s} = 205$  GeV.

The information from the four LEP experiments regarding the searches for  $e^+e^- \rightarrow hA$  is summarised in Table 2 which lists the predicted SM background and the events observed in the  $b\bar{b}b\bar{b}$ ,  $\tau^+\tau^-b\bar{b}$  and  $b\bar{b}\tau^+\tau^-$  channels and the 95% CL limits, expected and observed. (For the  $e^+e^- \rightarrow hZ$  process Table 1 is relevant.)

| Experiment:   | ALEPH       | DELPHI      | L3      | OPAL        |
|---|-------------|-------------|---------|-------------|
| <204.5 GeV: Integrated luminosity ( $pb^{-1}$ ):      | 10.6        | 9.0         | 9.4     | 9.5         |
| Backg. predicted / Evts. observed                     | 0.4 / 0     | 5.6 / 4     |         | 0.6/2       |
| $b\bar{b}b\bar{b}$ :                                  | 0.3 / 0     | 5.3 / 3     | 0.5 / 0 | 0.4/2       |
| $\tau^+\tau^-b\bar{b}$ and $b\bar{b}\tau^+\tau^-$ :   | 0.1 / 0     | 0.3 / 1     |         | 0.2/0       |
| 204.5-205.5 GeV: Integrated luminosity ( $pb^{-1}$ ): | 52.5        | 53.4        | 38.0    | 44.0        |
| Backg. predicted / Evts. observed                     | 2.1 / 2     | 30.3 / 40   |         | 2.9/2       |
| $b\bar{b}b\bar{b}$ :                                  | 1.3 / 1     | 28.5 / 39   | 2.2 / 6 | 2.0/2       |
| $\tau^+\tau^-b\bar{b}$ and $b\bar{b}\tau^+\tau^-$ :   | 0.8 / 1     | 1.8 / 1     |         | 0.9/0       |
| >205.5 GeV: Integrated luminosity ( $pb^{-1}$ ):      | 31.1        | 33.7        | 22.7    | 26.5        |
| Backg. predicted / Evts. observed                     | 1.2 / 3     | 19.7 / 24   |         | 1.8/0       |
| $b\bar{b}b\bar{b}$ :                                  | 0.8 / 3     | 18.6 / 23   | 1.4 / 0 | 1.2/0       |
| $\tau^+\tau^-b\bar{b}$ and $b\bar{b}\tau^+\tau^-$ :   | 0.4 / 0     | 1.1 / 1     |         | 0.6/0       |
| Total: Integrated luminosity ( $pb^{-1}$ ):           | 94.2        | 96.1        | 70.1    | 80.0        |
| Backg. predicted / Evts. observed                     | 3.7 / 5     | 55.6 / 68   |         | 5.4 / 4     |
| $b\bar{b}b\bar{b}$ :                                  | 2.4 / 4     | 52.4 / 65   | 4.1 / 6 | 3.7 / 4     |
| $\tau^+\tau^-b\bar{b}$ and $b\bar{b}\tau^+\tau^-$ :   | 1.3 / 1     | 3.2 / 3     |         | 1.7 / 0     |
| Events in all channels:                               | 3.7 / 5     | 55.6 / 68   | 4.1 / 6 | 5.4 / 4     |
| Limit exp.(median)/obs. for $m_h$ ( $GeV/c^2$ ):(*)   | 90.6 / 91.2 | 87.0 / 85.1 |         | 87.1 / 81.0 |
| Limit exp.(median)/obs. for $m_A$ ( $GeV/c^2$ ):(*)   | 91.0 / 91.6 | 88.5 / 86.7 |         | 87.9 / 81.2 |

Table 2: *Information related to searches of the four LEP experiments for the process  $e^+e^- \rightarrow hA$  at energies from 200 to 209 GeV (year 2000 data). In the L3 analysis the event selection, and thus the expected background and observed number of events, depend on the Higgs boson mass hypothesis; they are given here for  $m_h \approx m_A = 95$   $GeV/c^2$ . (\*)In the ALEPH publication the confidence level estimator used is different from the one used by the other collaborations.*

Plots of  $m_h + m_A$  for the candidate events of the four LEP experiments can be seen in Figure 5 for the  $\tau^+\tau^-b\bar{b}$  and  $b\bar{b}\tau^+\tau^-$  final states.

To search for a possible signal for the neutral Higgs bosons h and A, the MSSM parameters have been scanned according to the three benchmarks described in Appendix B. Each scan point is regarded as a hypothetical model, for which the procedure of calculating the test-statistic  $X$  and the confidence levels  $CL_b$ ,  $CL_{s+b}$ ,  $CL_s$  has been applied as in the SM case, with the inclusion of numerous additional search channels from the process  $e^+e^- \rightarrow hA$ .

## MSSM HIGGS - PRELIMINARY

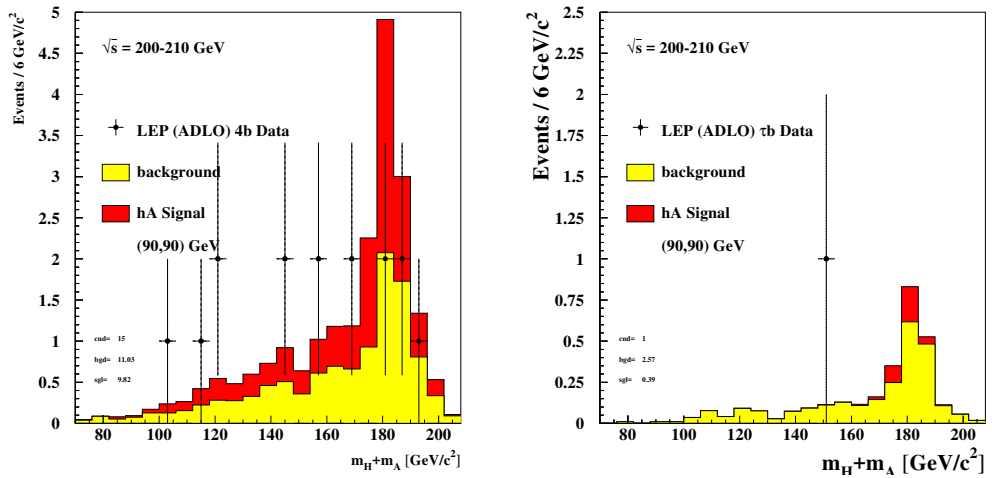


Figure 5:  $m_H + m_A$  for the MSSM candidate events from the four LEP experiments for the  $b\bar{b}b\bar{b}b\bar{b}$  and  $\tau^+\tau^-b\bar{b}b\bar{b}$  final states.

Figure 6 shows the test-statistic  $X$  (here  $Q$ ) for the  $m_h$ -*max* benchmark scan, for the particular case  $m_h \approx m_A$ , where only the  $e^+e^- \rightarrow hA$  process contributes, since  $\sin^2(\beta - \alpha) \approx 0$ . The heavy Higgs boson is kinematically out of reach for this benchmark scan and does not contribute. If there were a signal with  $m_h \approx m_A$ , then the test-statistic would have a minimum at the corresponding value of  $m_h + m_A$ . Negative values of the test-statistic show a preference of the data for the signal hypothesis, and positive values indicate a preference for the background hypothesis. The expectations are shown for the background and the signal hypothesis as functions of  $m_h + m_A$ , with one- and two- $\sigma$  bands on the signal expectation. While the test-statistic is nearly always below that expected for the background hypothesis, it remains positive over the range to which the combination of the experiments is sensitive to a signal.

Figure 7 illustrates the compatibility of the background hypothesis with the data, quantified with  $1 - CL_b$ . The figure illustrates  $1 - CL_b$  only for signal hypotheses for which  $m_h \approx m_A$ , and for  $\tan \beta > 20$ . The heavy Higgs boson  $H$  is taken to be too heavy to be produced at LEP for this figure. In two places there are excursions below the  $2\sigma$  line. The excess at  $m_h = m_A \approx 85 \text{ GeV}/c^2$  arises from earlier data [1]. For  $m_h = m_A \approx 90 \text{ GeV}/c^2$ , the candidates accumulate near the peak of the background from  $e^+e^- \rightarrow Z^0Z^0$  production. Also shown in the figure is the median expectation for  $1 - CL_b$  for a signal with  $m_h \approx m_A$ . A value of  $1 - CL_b$  below  $5.7 \times 10^{-7}$  would indicate a discovery with a significance of five standard deviations. If there were a signal with  $m_h + m_A = 173.6 \text{ GeV}/c^2$  and  $m_h \approx m_A$ , then LEP would discover it at the  $5\sigma$  level in 50% of possible experiments.

Figure 8 illustrates the outcome for  $CL_s$ , also for  $m_h \approx m_A$ , for  $\tan \beta > 20$ , which yields  $\cos^2(\beta - \alpha) \approx 1$ . This quantity tests the consistency of the data with the signal hypothesis as a function of  $m_h + m_A$ . The expected and observed 95% CL limits on  $m_h + m_A$  are 181.0 and  $187.2 \text{ GeV}/c^2$ . These numbers are not directly comparable with the limits obtained in more complete scans of the MSSM parameter space because the minimum sensitivity lies not on the curve  $m_h = m_A$ , but slightly above it.

Figure 9 is the two-dimensional generalisation of Figure 7 where the observed  $1 - CL_b$  is projected onto the  $(m_h, m_A)$  plane (the case of the  $m_h$ -*max* benchmark scan, see Appendix B, is shown). A first hint towards signal-like behaviour would manifest itself as an ‘island’ where  $1 - CL_b$  deviates by more than  $3\sigma$  from the background prediction. No excursions are seen at the  $3\sigma$  significance level, although there are three locations where the significance exceeds  $2\sigma$ . Two of these are on the  $m_h \approx m_A$  line, and the significance can be seen in Figure 7. The third region is only a little over  $2\sigma$  in significance. The most significant of the regions, that at  $m_h = m_A \approx 85 \text{ GeV}/c^2$ , has a value of  $1 - CL_b = 6.0 \times 10^{-3}$ , and results from the combination of earlier data. Data taken in 2000 do not enhance the significance of this region. A Monte Carlo study was performed to investigate the probability of observing small values of  $1 - CL_b$  in the region of the  $(m_h, m_A)$  plane that was unexcluded for the combination of September 1999 [13], and which contains the three regions of small  $1 - CL_b$ . It was found that the probability of obtaining  $1 - CL_b \leq 6.0 \times 10^{-3}$  anywhere in the region was 38%. Hence no evidence for a signal of new physics is inferred from the results of this scan.

## MSSM HIGGS - PRELIMINARY

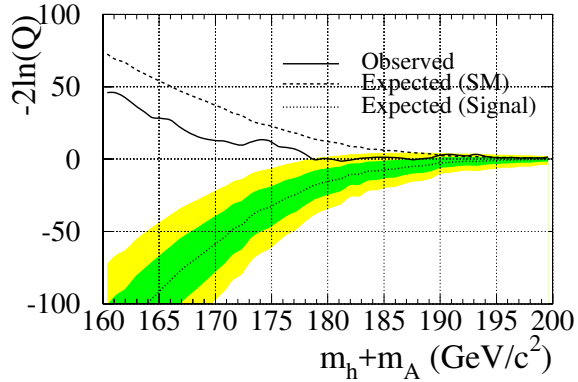


Figure 6: The negative log-likelihood ratio (test-statistic) as a function of  $m_h + m_A$ . The dashed line shows the expectation for the background-only hypothesis and the full line the values computed from the observed results. The dotted line and the shaded areas show the central value and the  $1\sigma$  and  $2\sigma$  probability bands for the signal at the “true” mass sum.

## MSSM HIGGS - PRELIMINARY

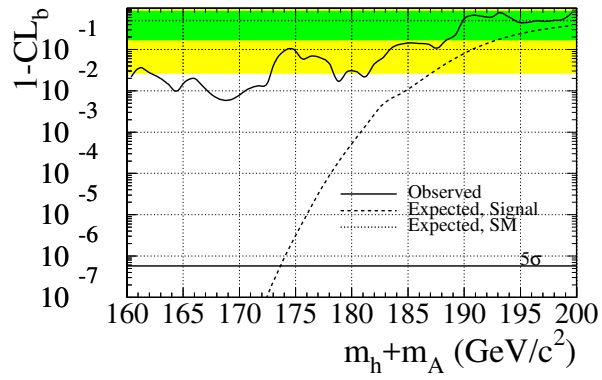


Figure 7: The confidence level  $CL_b$  as a function of  $m_h + m_A$ , for the  $m_h$ -max benchmark and the particular case  $m_h \approx m_A$  (where only the  $e^+e^- \rightarrow hA$  process contributes since  $\sin^2(\beta - \alpha) \approx 0$ ). The straight dotted line at 50% and the shaded bands represent the median result and the symmetric  $1\sigma$  and  $2\sigma$  probability bands expected in the absence of a signal. The solid curve is the observed result and the dashed curve shows the median result expected for a signal when tested at the “true” mass sum. The horizontal line at  $5.7 \times 10^{-7}$  indicates the level for a  $5\sigma$  discovery.

## MSSM HIGGS - PRELIMINARY

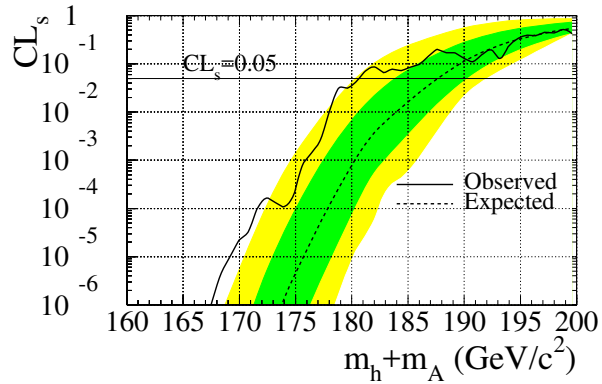


Figure 8: The confidence level  $CL_s$  as a function of  $m_h$ , for the  $m_h$ -max benchmark and the particular case  $m_h \approx m_A$  (where only the  $e^+e^- \rightarrow hA$  process contributes since  $\sin^2(\beta - \alpha) \approx 0$ ). The solid curve is the observed result, the dashed curve the median result expected in the absence of a signal. The shaded areas represent the symmetric  $1\sigma$  and  $2\sigma$  probability bands of  $CL_s$  in the absence of a signal. The intersection of the curves with the horizontal line at  $CL_s = 0.05$  give the limit on  $m_h + m_A$  at the 95% confidence level.

## MSSM HIGGS - PRELIMINARY

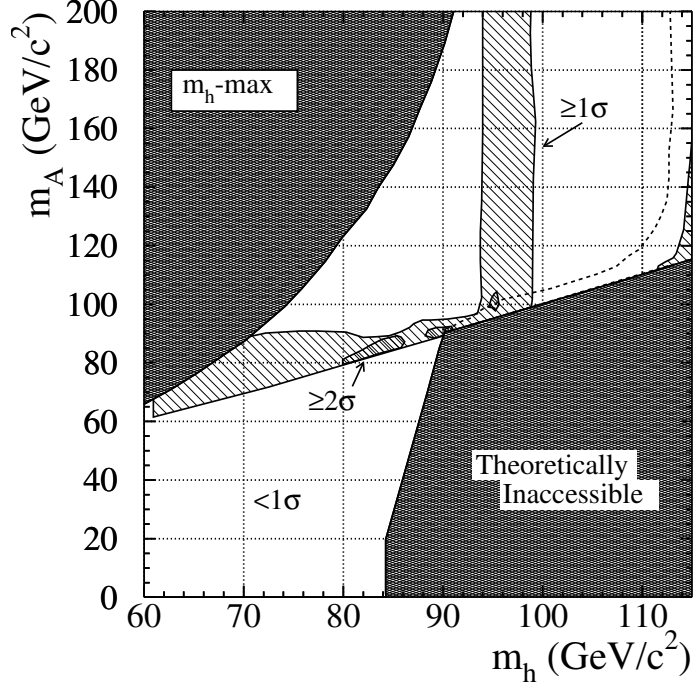


Figure 9: *Distribution of the confidence level  $1 - CL_b$  for the  $m_h$ -max benchmark, projected onto the  $(m_h, m_A)$  plane. In the white domain the observation either shows a deficit or is less than  $1\sigma$  above the background prediction; in the domains labeled  $\geq 1\sigma$  and  $\geq 2\sigma$ , the observation is above the prediction by the indicated amount. There are no domains for which the observation exceeds the prediction by more than  $3\sigma$ .*

Confidence levels are computed using the signal models defined by the three benchmark scans of Appendix B and 95% CL exclusion limits are derived in the corresponding MSSM parameter spaces. These are shown in Figures 10, 11, and 12 for the *no-mixing*,  $m_h$ -max and *large- $\mu$*  benchmarks. The limits are presented for  $\tan\beta > 0.4$  and in three parameter projections,  $(m_h, m_A)$ ,  $(m_h, \tan\beta)$ , and  $(m_A, \tan\beta)$ . Besides the limits obtained from the data, the ones expected on the basis of background Monte Carlo experiments are also shown. For the  $m_h$ -max and *no-mixing* scans, the  $\tan\beta$  axis is restricted to a maximum value of 30; the Higgs boson can have width exceeding the experimental resolution for larger  $\tan\beta$ , requiring additional Monte Carlo estimates of the reconstructed mass distributions. The decay widths of the observable Higgs bosons remain small in the *large- $\mu$*  scenario;  $\tan\beta$  is shown up to 50 for the *large- $\mu$*  scenario.

In the *no-mixing* scenario, an unexcluded feature appears<sup>2</sup> at low  $\tan\beta$ . For  $m_h > 60 \text{ GeV}/c^2$  and  $m_A < 10 \text{ GeV}/c^2$ , the decay  $h \rightarrow AA$  dominates, and the  $A$  cannot decay into  $b\bar{b}$  because

<sup>2</sup>This feature did not appear in previous preliminary work because of a mistake in the handling of branching fractions during the combination procedure.

it is kinematically unavailable. The branching ratio  $\text{Br}(h \rightarrow b\bar{b})$  rises with decreasing  $m_h$  in this scenario for  $m_A < 10 \text{ GeV}/c^2$ , and becomes large enough to provide exclusion for  $m_h < 60 \text{ GeV}/c^2$ . For  $m_h \approx 85 \text{ GeV}/c^2$  at low values of  $\tan\beta$  (between 0.4 and 0.45),  $h \rightarrow AA$  dominates, and  $\text{Br}(A \rightarrow b\bar{b})$  is suppressed. These regions may be searched in the future using flavour-independent searches (the  $A$  can decay into charm pairs or gluons), and the sensitivity of the HZ channels can be optimised for  $m_h < 85 \text{ GeV}/c^2$ .

Results in the *large- $\mu$*  scenario are presented here for the first time. The largest value of  $m_h$  in the scan is  $107.9 \text{ GeV}/c^2$ , well within the reach of the LEP experiments this year. Nonetheless, there are regions for which  $\sin^2(\beta - \alpha)$  is small and  $e^+e^- \rightarrow hA$  production is kinematically suppressed. As a special case for this scenario, the heavy Higgs boson is within kinematic reach and the signal from it can be used to exclude such points. What remains unexcluded are points for which  $\text{Br}(h \rightarrow b\bar{b})$  is suppressed, giving way to charm quarks, gluons, and  $W^+W^-$  decays of the  $h$ , with the  $\tau^+\tau^-$  decays not always enhanced over their standard model values. These points have  $m_h$  very near the upper bound allowed by the scenario, so the tau channels alone cannot exclude them. ALEPH has developed [6] flavour-independent missing-energy and lepton channels and included them for combination; this provides some constraints on the size of the remaining unexcluded region, although the separation of signal from background is not as good as it is for the case  $h \rightarrow b\bar{b}$ . Numerical limits on  $m_h$ ,  $m_A$ , and  $\tan\beta$  are not provided for this example scan; a small change in the model parameters can easily push the maximum  $m_h$  beyond the kinematic reach of LEP. Its purpose is to identify points which are difficult to exclude because of the decay branching ratios.

## MSSM HIGGS - PRELIMINARY

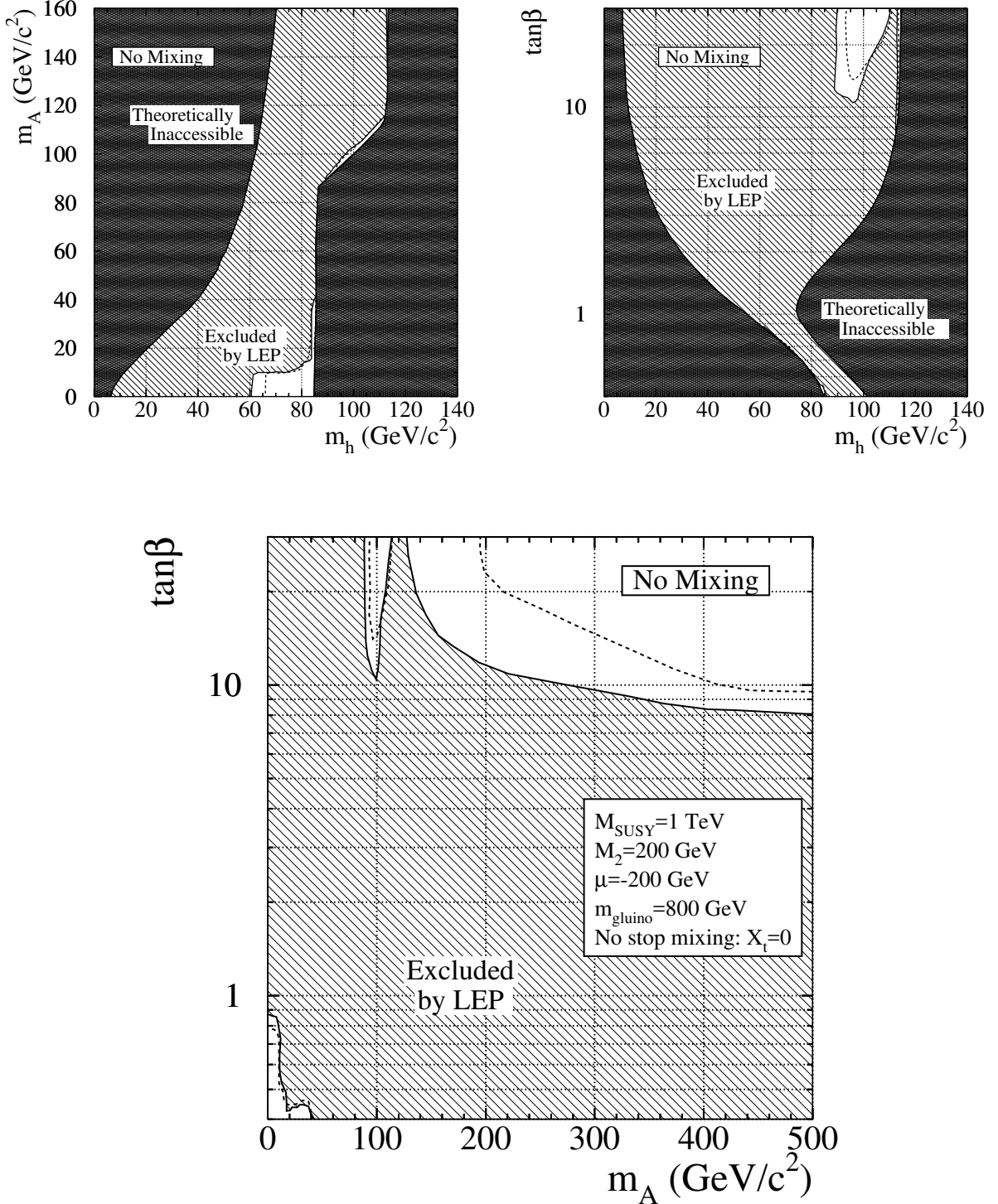


Figure 10: The 95% CL bounds on  $m_h$ ,  $m_A$  and  $\tan\beta$ , for the no-mixing benchmark, from combining the data of the four LEP experiments taken at 200 to 210 GeV with earlier data taken at lower energies. The full lines represent the actual observation and the dashed lines the limits expected on the basis of ‘background only’ Monte Carlo experiments. Upper left: projection ( $m_h$ ,  $m_A$ ) for  $\tan\beta > 0.4$ ; upper right: projection ( $m_h$ ,  $\tan\beta$ ); lower part: projection ( $m_A$ ,  $\tan\beta$ ).

## MSSM HIGGS - PRELIMINARY

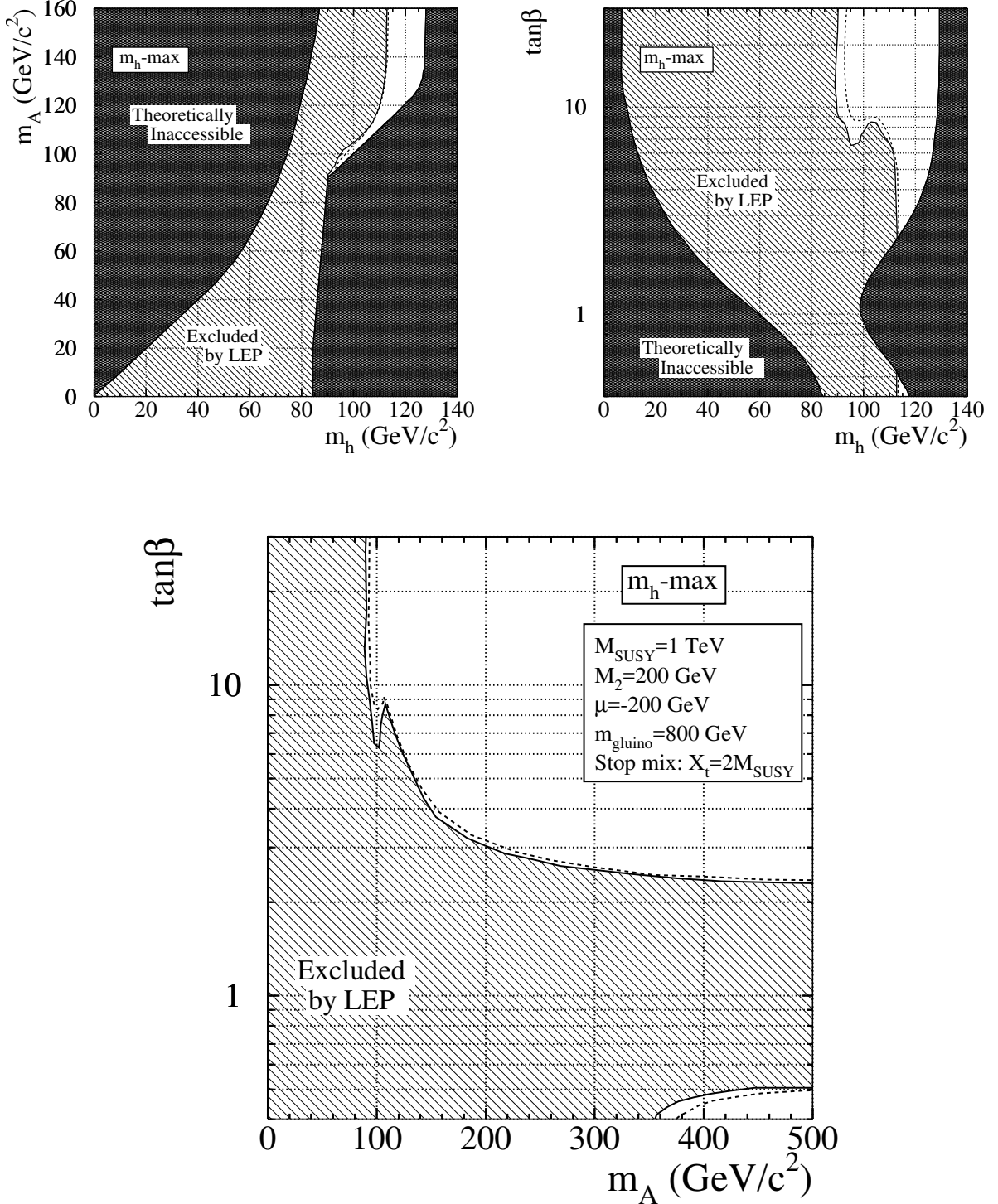


Figure 11: The 95% CL bounds on  $m_h$ ,  $m_A$  and  $\tan\beta$ , for the  $m_h$ -max benchmark, from combining the data of the four LEP experiments taken at 200 to 210 GeV with earlier data taken at lower energies. The full lines represent the actual observation and the dashed lines the limits expected on the basis of ‘background only’ Monte Carlo experiments. Upper left: projection ( $m_h$ ,  $m_A$ ) for  $\tan\beta > 0.4$ ; upper right: projection ( $m_h$ ,  $\tan\beta$ ); lower part: projection ( $m_A$ ,  $\tan\beta$ ).

## MSSM HIGGS - PRELIMINARY

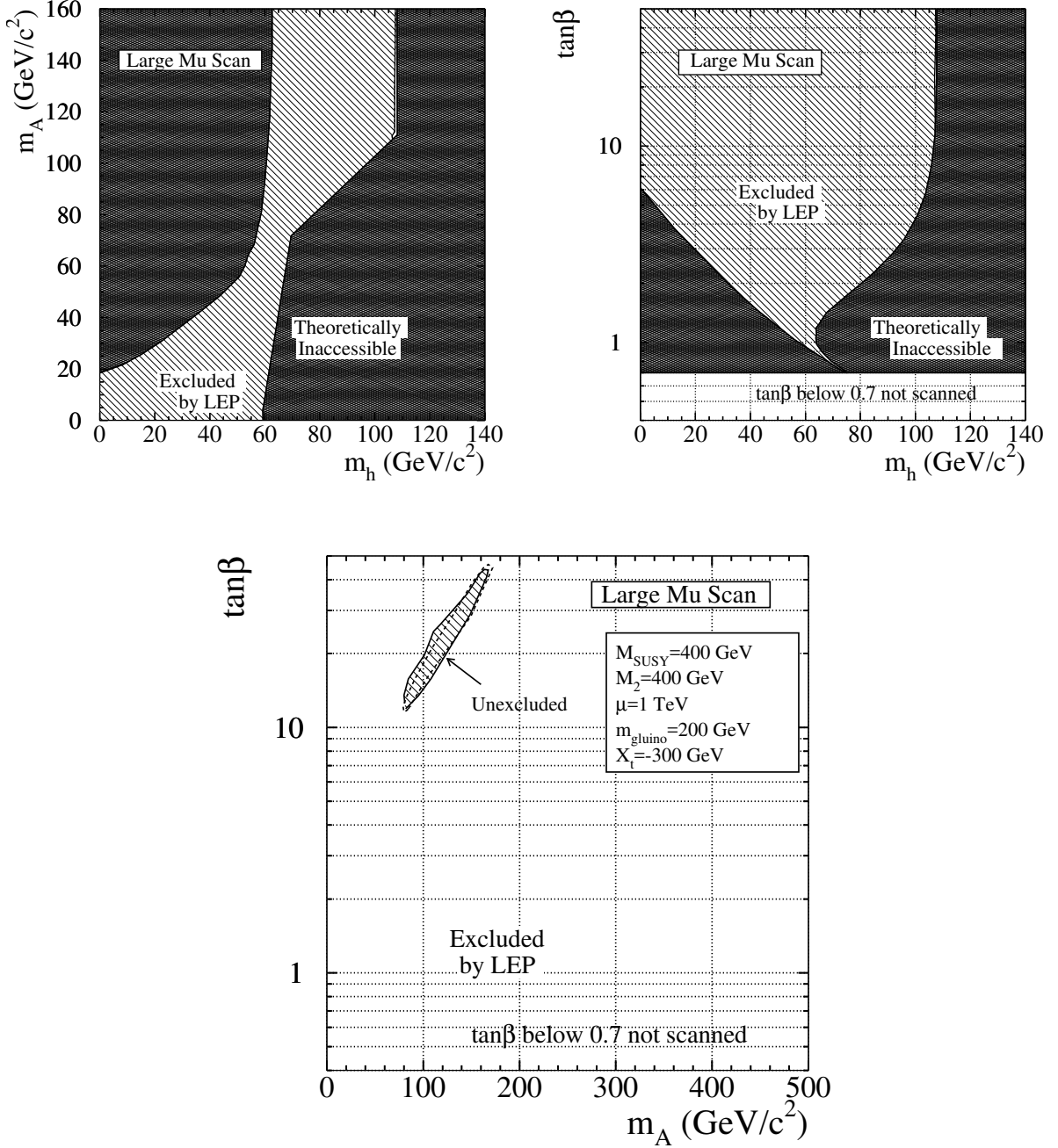


Figure 12: The 95% CL bounds on  $m_h$ ,  $m_A$  and  $\tan\beta$ , for the large- $\mu$  benchmark, from combining the data of the four LEP experiments taken at 200 to 210 GeV with earlier data taken at lower energies. The full lines represent the actual observation and the dashed lines the limits expected on the basis of ‘background only’ Monte Carlo experiments. Upper left: projection ( $m_h$ ,  $m_A$ ) for  $\tan\beta > 0.7$ ; upper right: projection ( $m_h$ ,  $\tan\beta$ ); lower part: projection ( $m_A$ ,  $\tan\beta$ ). The first two projections have very small unexcluded regions for  $m_h \approx 108$  GeV/c $^2$ , near the edges of the regions which are allowed in the scenario. The region which is unexcluded is so because the branching ratio of  $h \rightarrow b\bar{b}$  nearly vanishes for these points.

The mass limits obtained for the the  $m_h$ -max and *no-mixing* scenarios are presented in Table 3.

|  | no-mixing          | $m_h$ -max         |
|--|--------------------|--------------------|
| Limits for $m_h$ ( $\text{GeV}/c^2$ )<br>expected (median) :<br>observed : | 92.4<br>90.4       | 92.2<br>90.5       |
| Limits for $m_A$ ( $\text{GeV}/c^2$ )<br>expected (median):<br>observed :  | 92.9<br>90.5       | 92.8<br>90.5       |
| Exclusion in $\tan \beta$<br>expected (median):<br>observed :              | 0.8-8.6<br>0.9-7.7 | 0.5-2.3<br>0.5-2.3 |

Table 3: *Combined 95% confidence level MSSM limits for  $m_h$  and  $m_A$  and excluded ranges in  $\tan \beta$  for the  $m_h$ -max and no-mixing scenarios. The limits on  $m_h$  and  $m_A$  are valid for  $\tan \beta > 0.9$  in the no-mixing scan and for  $\tan \beta > 0.4$  in the  $m_h$ -max scan. The  $\tan \beta$  limits are valid for top masses less than  $174.3 \text{ GeV}/c^2$ . The quoted limits include the effect of the systematic errors on the experimental results and their correlations. No theoretical uncertainties from unknown higher-order corrections are taken into account.*

In obtaining the limits quoted in Table 3, systematic errors have been taken into account together with their correlations between experiments, data sets at different energies and between search channels. Their inclusion has the effect of decreasing the expected mass limits by about  $300 \text{ MeV}/c^2$ . The model predictions are made as described in Appendix B, and no uncertainties due to unknown higher-order corrections are taken into account in deriving the limits.

As a cross-check of the confidence level calculation procedures, the expected and observed limits have been calculated independently, using another test-statistic (Method B in [10]). The observed and expected limits are within  $\pm 1 \text{ GeV}/c^2$  of the values in Table 3.

Based on the above results, we quote the following preliminary 95% CL lower bounds:  $m_h > 90.5 \text{ GeV}/c^2$ ,  $m_A > 90.5 \text{ GeV}/c^2$ . These bounds are valid for  $\tan \beta > 0.9$ , and for top masses less than  $174.3 \text{ GeV}/c^2$ . The ranges of  $\tan \beta$  excluded for other top mass ranges are given in Table 4.

## 4 Combined searches for the charged Higgs bosons

Charged Higgs bosons are predicted by extensions of the SM with two Higgs field doublets (2HD models) of which the MSSM is a particular case with supersymmetry. At LEP2 energies charged Higgs bosons are expected to be produced mainly through the process  $e^+e^- \rightarrow H^+H^-$ .

| Top quark mass:           | $\leq 169.2 \text{ GeV}/c^2$ | $\leq 174.3 \text{ GeV}/c^2$ | $\leq 179.4 \text{ GeV}/c^2$ |
|---------------------------|------------------------------|------------------------------|------------------------------|
| Exclusion in $\tan \beta$ |                              |                              |                              |
| No mixing :               | 0.9-10                       | 0.9-7.7                      | 0.9-5.5                      |
| $m_h\text{-max:}$         | 0.4-2.9                      | 0.5-2.3                      | 0.7-1.9                      |

Table 4: *Exclusion in  $\tan \beta$  at the 95% confidence level for various top mass ranges. The bound at 0.4 in the  $m_h\text{-max}$  limit for  $m_t=169.2 \text{ GeV}/c^2$  is due to the  $\tan \beta$  range of the scan.*

In the MSSM and at tree-level the  $H^\pm$  is constrained to be heavier than the  $W^\pm$  bosons but loop corrections can drive the mass to lower values. Since the sensitivity of current searches is limited to the range below  $m_{W^\pm}$  due to the background from  $e^+e^- \rightarrow W^+W^-$ , any signal for  $H^+H^-$  would indicate either new physics beyond the MSSM or a rather extreme set of MSSM parameter values.

The present searches for charged Higgs bosons are placed in the general context of 2HD models where the mass is not constrained. At tree level the production cross-section is fully determined by the  $H^\pm$  mass [14]; here they are provided by HZHA Version 3. The searches are carried out under the assumption that the two decays  $H^+ \rightarrow c\bar{s}$  and  $H^+ \rightarrow \tau^+\nu$  exhaust the  $H^+$  decay width; however, the relative branching ratio is not predicted. Thus, the searches encompass the following  $H^+H^-$  final states:  $(c\bar{s})(\bar{c}s)$ ,  $(\tau^+\nu)(\tau^-\bar{\nu})$  and the mixed mode  $(c\bar{s})(\tau^-\bar{\nu}) + (\bar{c}s)(\tau^+\nu)$ . The combined search results are presented as a function of the branching ratio  $B(H^+ \rightarrow \tau^+\nu)$ .

Details of the searches carried out by the four LEP experiments, using the data collected at energies between 200 and 209 GeV (year 2000 data), can be found in [15]. These are summarised in Table 5, together with the 95% CL lower bounds, expected and observed. In the table we quote the mass limits obtained individually by the four experiments, separately for  $B(H^+ \rightarrow \tau^+\nu) = 0, 1$ , and a limit independent of the branching ratio.

Plots of the candidate masses can be seen in Figure 13 for the hadronic and semileptonic final states.

## CHARGED HIGGS - PRELIMINARY

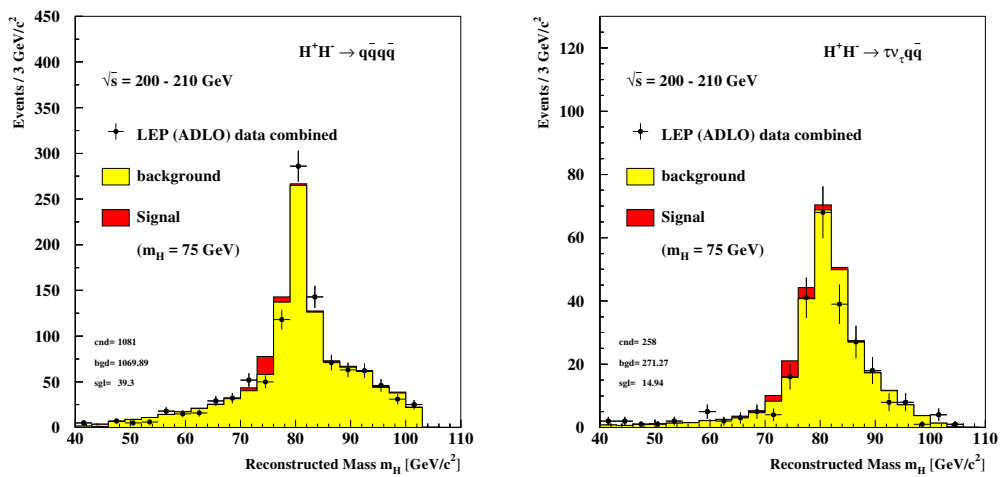


Figure 13: *Reconstructed mass for candidate events in the charged Higgs searches by the 4 LEP experiments..*

In order to search for a possible signal, the test mass  $m_{H^\pm}$  has been scanned. The test-statistic  $X = -2\ln(Q) = \Delta\chi^2$  versus the test mass  $m_{H^\pm}$  is shown in Figure 14, separately for the branching ratio  $B(\tau^+\nu)$  fixed to 1, 0.5 and 0. The observation is everywhere well within the 2 sigma band corresponding to the background only hypothesis. The test-statistic is never negative, apart in regions of masses higher than the ones where we have sensitivity, showing clearly that no signal is seen.

Figure 15 shows the background confidence level  $1 - CL_b$  as a function of  $m_{H^\pm}$ , expected and observed, for  $B(\tau^+\nu)=1, 0.5$  and 0. The observation is mostly within the light-shaded  $\pm 2\sigma$  bands of the background prediction, except for some low mass regions, from 60 to 67  $\text{GeV}/c^2$  at  $B(\tau^+\nu)=0.5$  and around 66  $\text{GeV}/c^2$  at  $B(\tau^+\nu)=1$  that never reach the  $3\sigma$  level and are far from the expectation for a signal.

The mass limits expected and observed are shown in Figure 16. To obtain the limit lines, the branching ratio  $B(\tau^+\nu)$  has been scanned in steps of 0.05, and the limit setting procedure outlined in Appendix A repeated for each step.

The combined 95% CL bounds are listed in Table 6 for  $B(\tau^+\nu)=0, 1$ , and for the weakest limit obtained for any value of  $B(\tau^+\nu)$ . Taking the lowest of the observed limits from Table 6, we choose to quote a 95% CL lower bound of 77.4  $\text{GeV}/c^2$  for the mass of the charged Higgs boson.

These limits have been obtained with the systematic errors taken into account. The error treatment has shifted the observed mass limits downwards by 1000, 700, and 100  $\text{MeV}/c^2$  for  $B(\tau^+\nu)=0, 0.5$  and 1, respectively.

As a cross-check of the confidence level calculation procedures, the expected and observed limits have been calculated independently, using another test-statistic (Method C in [10]). The limits were within  $\pm 1.2 \text{ GeV}/c^2$  of the quoted values.

| Experiment:                                  | ALEPH     | DELPHI    | L3        | OPAL        |
|--|-----------|-----------|-----------|-------------|
| Total: Int. luminosity ( $\text{pb}^{-1}$ ): | 90.5      | 74        | 92.1      | 87.5        |
| Backg. exp. / Events obs. (*)                |           |           |           |             |
| $(c\bar{s})(\bar{c}s)$ :                     | 452.8/438 | 127.2/147 | 375.0/391 | 193.6/171   |
| $(c\bar{s})(\tau^+\nu)$ :                    | 49.2/50   | 72.5/ 59  | 71.2/77   | 92.4/83     |
| $(\tau^+\nu)(\tau^-\bar{\nu})$ :             | 9.6/4     | 8.8/ 12   | 16.9/16   | —           |
| Events in all channels:                      | 511.6/492 | 208.5/218 | 463.1/484 | 286.0/254   |
| Limit exp.(median)/ observed (*)             |           |           |           |             |
| for $B=0$ :                                  | 78.4/80.9 | 76.5/76.7 | 77.0/77.3 | 77.2 / 75.4 |
| for $B=1$ :                                  | 86.4/82.8 | 86.5/85.0 | 81.4/81.6 | 86.1 / 84.3 |
| for any $B$ :                                | 77.0/76.4 | 74.4/75.0 | 76.1/66.3 | 75.6 / 70.5 |

Table 5: *Individual search results for the  $e^+e^- \rightarrow H^+H^-$  final states. The numbers of events correspond to the data sets taken at energies between 200 and 209 GeV (year 2000 data). (\*) The OPAL selection is mass-dependent; the numbers are given here for  $m_{H^\pm} = 80 \text{ GeV}/c^2$ . Also, the OPAL systematic uncertainty is handled conservatively by reducing the subtractable background by 1 standard deviation.*

## CHARGED HIGGS -PRELIMINARY

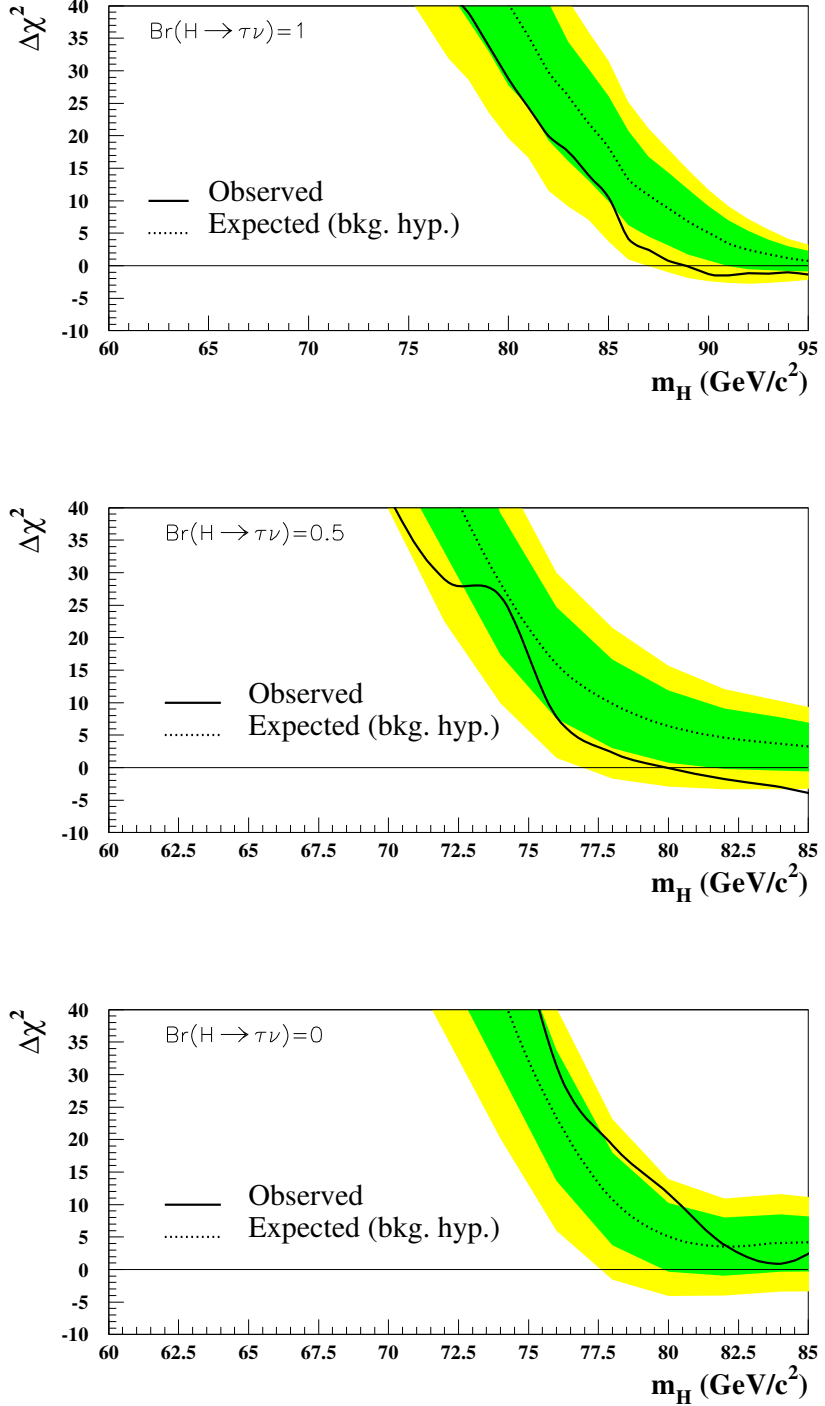


Figure 14: The  $\Delta\chi^2$  as a function of  $m_{H^\pm}$ , separately for  $B(\tau^+\nu)=0$ ,  $0.5$  and  $1$ . In each case, the dotted line shows the expectation for the background-only hypothesis and the full line the values computed from the observed results. The shaded areas show the symmetric  $1\sigma$  and  $2\sigma$  probability bands for the background hypothesis.

## CHARGED HIGGS - PRELIMINARY

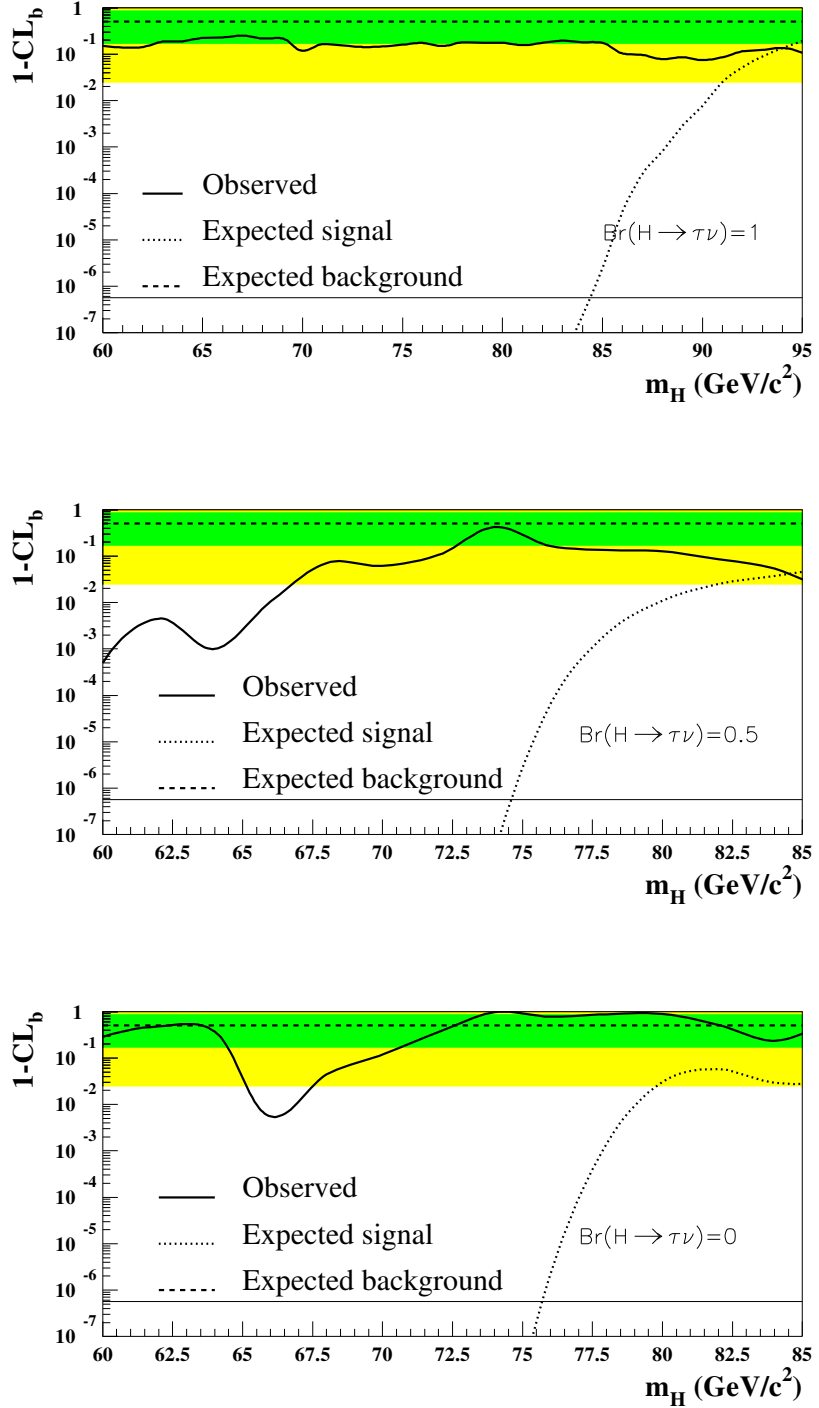


Figure 15: The confidence level  $1-CL_b$  as a function of  $m_{H^\pm}$ , for the branching ratio  $B(H^+ \rightarrow \tau^+ \nu) = 0$ , 0.5 and 1 (separate plots). The straight horizontal line at 50% and the shaded bands represent the mean result and the symmetric  $1\sigma$  and  $2\sigma$  probability bands expected in the absence of a signal. The solid curve is the observed result and the dashed curve shows the median result expected for a signal when tested at the “true” mass.

## CHARGED HIGGS - PRELIMINARY

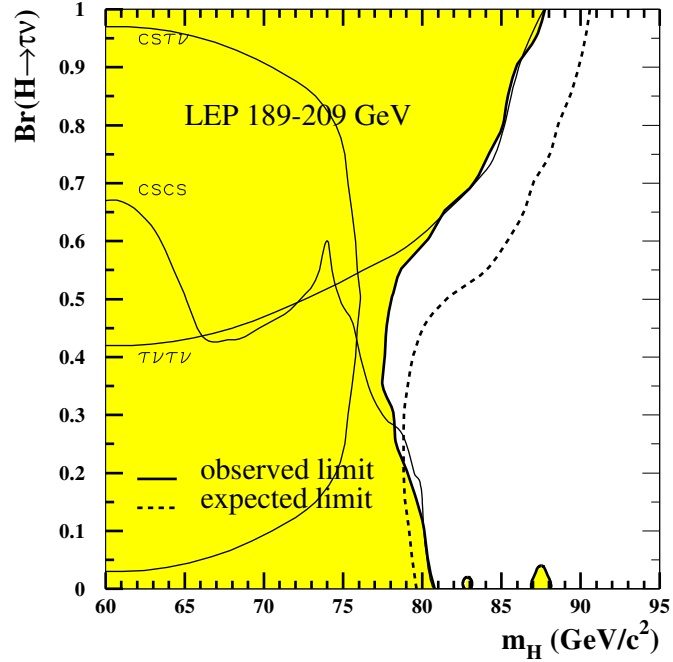


Figure 16: The 95% CL bounds on  $m_{H^\pm}$  as a function of the branching ratio  $B(H^+ \rightarrow \tau^+ \nu)$ , combining the data collected by the four LEP experiments at energies from 183 to 202 GeV. The expected exclusion limits are indicated by the dashed line and the observed limits by the heavy full line. The light full lines show the observed limits channel by channel.

|  | Mass limit in $\text{GeV}/c^2$ (95% CL) |
|--|---|
| $B(\tau^+\nu)=0$<br>Limit expected (median) :<br>Limit observed :  | 79.7<br>80.8, “islands”                 |
| $B(\tau^+\nu)=1$<br>Limit expected (median) :<br>Limit observed :  | 90.5<br>87.7                            |
| Any $B(\tau^+\nu)$<br>Limit expected (median):<br>Limit observed : | 78.5<br>77.4                            |

Table 6: *The combined 95% CL lower bounds for the mass of the charged Higgs boson, expected and observed, for fixed and values of the branching ratio  $B(\tau^+\nu)$  and for the  $B(\tau^+\nu)$  giving the weakest limit.*

## 5 Combined search for the process $h^0 \rightarrow \gamma\gamma$

In the minimal Standard Model, the single Higgs boson can decay into two photons via a quark- or W-boson loop [17]. The rate is too small for observation at existing accelerators even for a kinematically accessible Higgs boson, but other theoretical models can accommodate large  $h^0 \rightarrow \gamma\gamma$  branching ratios [18]. In the 2-Higgs-Doublet Model of Type I [19], for instance, a certain value of the parameter  $\alpha$  causes the  $h^0$  to couple only to bosons [20]. The class of “fermiophobic” Higgs models includes the more general “Bosonic” Higgs model [21], and Higgs-Triplet models [22] where the particles formed from the triplet fields are fermiophobic. For  $m_h < 90$  GeV, the fermiophobic Higgs decays primarily into  $\gamma\gamma$ .

The four LEP experiments search for events having two energetic, isolated photons. In addition, the  $Z^0$  decay products are either classified, or, in the case of  $Z^0 \rightarrow \nu\bar{\nu}$ , acoplanarity on the photons is required. For the 2000 data, the ALEPH analysis is “global” (the final states are not listed separately). The analysis procedures of the four LEP experiments producing the inputs for the present combination are described in individual documents [5, 23, 24, 25, 26]; we merely summarise the results in Table 7.

As a benchmark for exclusion of Higgs bosons in fermiophobic models, we consider an  $h^0$  produced in  $e^+e^- \rightarrow h^0 Z^0$  with Standard model production cross section and with the partial width for  $h^0 \rightarrow \gamma\gamma$  given by the Standard Model, but with the dfermion partial widths set to zero. We have examined two methods [2, 27] of calculating this branching fraction. As [27] gives slightly more conservative limits, it is the one we use here. Figure 17 shows the combined data for the four LEP experiments, together with the expected signal for the “benchmark” fermiophobic Higgs boson of mass 100 GeV. In two cases, data which exist in publications have not yet been included in the combination. The ALEPH input functions currently have no background estimate for the 88-189 GeV data, and the background estimate for the 192-210 GeV data is not subtractable. Therefore, ALEPH results cannot be combined into a calculation of  $CL_b$ . Likewise, the OPAL leptonic channel background for the 88-183 GeV data is not available in the standard input format and is therefore excluded from combinations. The combined data from DELPHI, L3, and OPAL yield the distribution of  $1 - CL_b$  shown in Figure 18; there is no indication of new physics. The 95% confidence level upper limit for  $BR(h^0 \rightarrow \gamma\gamma)$  incorporating all the combined ADLO data in Table 7 is shown in Figure 19. A benchmark lower mass limit for fermiophobic Higgs bosons is obtained where the limit curve crosses the benchmark  $B_{\gamma\gamma}(m_h)$  curve; for the combined ADLO data this limit is 106.4 GeV.

| Experiment:   | ALEPH                                | DELPHI                       | L3                             | OPAL   |
|---|--------------------------------------|------------------------------|--------------------------------|--|
| 200-209 GeV (Y2000) Luminosity: :<br>Backg. predicted / Evt. observed<br>Hadronic:<br>Leptonic:<br>Missing-energy:<br>Global: | 94 $pb^{-1}$<br>—<br>—<br>—<br>2.2/2 | —<br>—<br>—<br>—             | —<br>—<br>—<br>—               | 84 $pb^{-1}$<br>2.6/4<br>3.3/7<br>2.2/1<br>— |
| 192-202 GeV (Y1999):<br>Backg. predicted / Evt. observed<br>Hadronic:<br>Leptonic:<br>Missing-energy:<br>Global:              | —<br>—<br>—<br>5.8/6                 | 27.7/27<br>—<br>7.3/7<br>—   | 12.5/14<br>—<br>—<br>—         | 10.9/15<br>9.2/5<br>7.6/3<br>—               |
| 189 GeV (Y1998):<br>Backg. predicted / Evt. observed<br>Hadronic:<br>Leptonic:<br>Missing-energy:                             | —<br>—<br>—                          | 24.7/26<br>—<br>5.6/8        | 16.2/10<br>2.5/5<br>4.3/3      | 9.0/10<br>8.9/7<br>7.1/5                     |
| 88-183 GeV (Y1990-97):<br>Backg. predicted / Evt. observed<br>Hadronic:<br>Missing-energy:                                    | —<br>—                               | —<br>—                       | —<br>—                         | 170.9/178<br>9.7/10                          |
| Total:<br>Backg. predicted / Evt. observed<br>Hadronic:<br>Leptonic:<br>Missing-energy:<br>Global:                            | —<br>—<br>—<br>8.0/8                 | 52.4/53<br>—<br>12.9/15<br>— | 28.7/24<br>2.5/5<br>4.3/3<br>— | 185.3/197<br>21.4/19<br>20.5/14<br>—         |
| Events in all channels  | 8.0/8                                | 65.3/68                      | 35.5/32                        | 227.2/230                                    |
| Limit ( $GeV/c^2$ ) exp. (median) at 95% CL:  | 102.0                                | 97.5                         | 98.3                           | 103.5  |
| Limit ( $GeV/c^2$ ) observed at 95% CL:   | 102.7                                | 96.1                         | 99.9                           | 103.1  |
| Combined Limit ( observed / expected):  |                                      |                              | 106.4 / 105.6                  |  |

Table 7: *Information related to the searches of the four LEP experiments for the process  $H \rightarrow \gamma\gamma$  at energies between 88 and 209 GeV.*

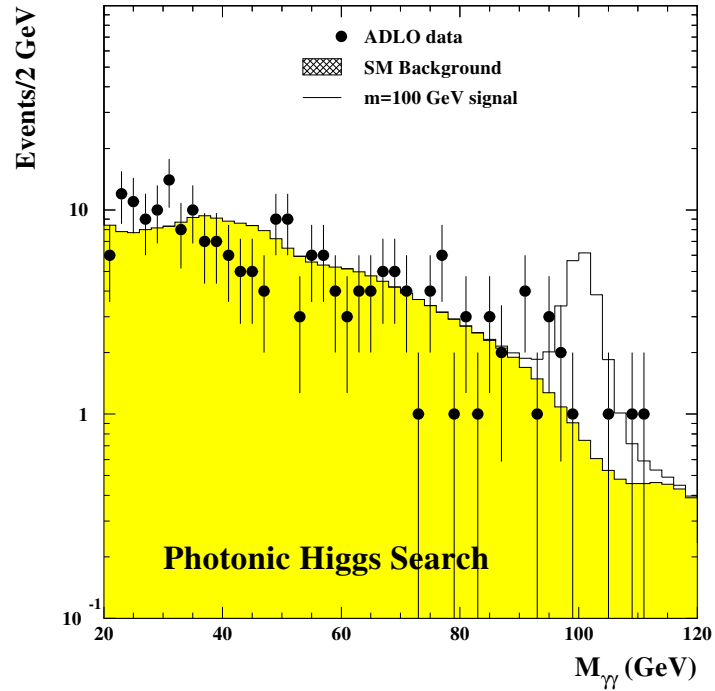


Figure 17: Distribution of the diphoton mass in the in the  $h^0 \rightarrow \gamma\gamma$  search. All search channels are included. Data are shown as points with error bars. Background simulation is shown as a histogram showing the contributions from the four LEP experiments. Also shown is the benchmark signal for  $m_h = 100$  GeV.

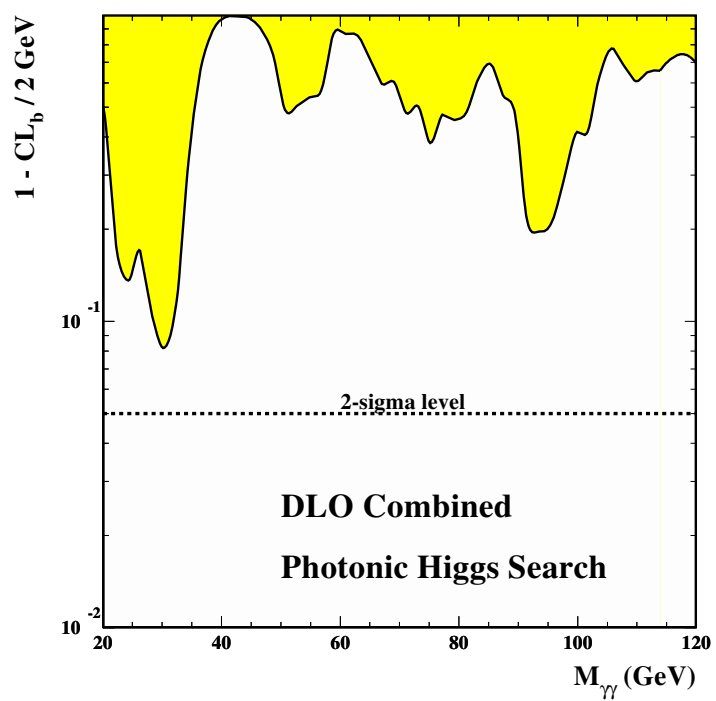


Figure 18: Distribution of  $1 - CL_b$  for the D,L,O combined data in the  $h^0 \rightarrow \gamma\gamma$  search.

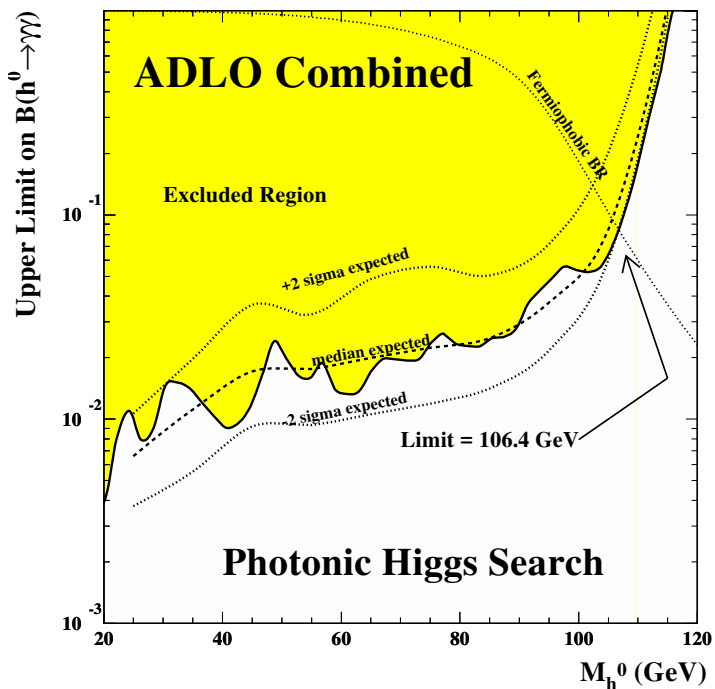


Figure 19: 95% confidence level upper limit on the diphoton branching fraction for a Standard Model Higgs boson production rate. The shaded region is excluded; The dashed line is the predicted benchmark diphoton branching fraction assuming  $B(h^0 \rightarrow f\bar{f})=0$ . The intersection of the dotted line with the exclusion curve gives a lower limit of 106.4 GeV for the fermiophobic Higgs model. Also shown (dotted lines) are the median expected limit and the 95% confidence level zone for the expected limit.

## 6 Combined searches for ‘invisible’ Higgs decays

The Higgs may not make its presence obvious. For instance, if there were a neutralino decay kinematically available it would be likely to dominate the Higgs decay modes, and such decays would be invisible at LEP. Majoron models also produce dominantly invisible Higgs decay modes. However, if Higgs bosons are produced through the normal Higgs-strahlung process then the  $Z^0$  can be detected in the normal way, and the presence of the Higgs inferred. The reconstructed Higgs boson mass is taken to be the mass of the invisible system recoiling from the visible  $Z^0$  decay products and does not depend on model assumptions aside from the assumption of Higgsstrahlung production.

Searches with this strategy are considered by the LEP Higgs working group for the first time here. Only 3 experiments, ALEPH, DELPHI and OPAL, had data in a suitable form for this combination, and of these only ALEPH and OPAL produced data from the 2000 run. ALEPH results from 189 to 208  $\text{GeV}/c^2$ , OPAL from 183 to 208, and DELPHI from 183 to 202  $\text{GeV}/c^2$  were included. The analysis procedures of the three LEP experiments producing the inputs for the present combination are described in individual documents [28, 29, 30]; we merely summarise the results in Table 8. All events which make an entry to Table 8 are used below in the calculation of confidence levels and in the limit-setting procedure. For the OPAL limit in the table,  $101.1 \text{ pb}^{-1}$  have been used; however, for the LEP-combination, only  $74.7 \text{ pb}^{-1}$  were available in the standard inputs.

The reconstructed candidate masses is shown in Figure 20 for the data, signal estimations, and Standard Model backgrounds, for the combination given in this paper.

## INVISIBLE HIGGS - PRELIMINARY

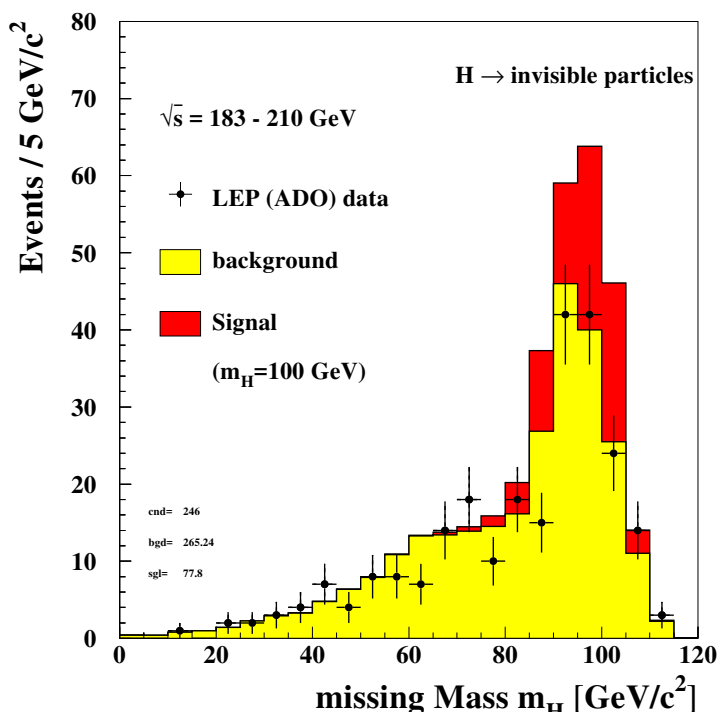


Figure 20: Missing mass for candidate events from the invisible Higgs boson final state search. The ALEPH analysis is mass dependent; the data for  $m_h=100 \text{ GeV}/c^2$  has been used in this plot.

| Experiment:  | ALEPH    | DELPHI | L3 | OPAL      |
|--|----------|--------|----|-----------|
| Total 2000 Integrated luminosity ( $\text{pb}^{-1}$ ): | 94.2     | –      | –  | 101.1     |
| Backg. predicted / Evts. observed                      |          |        |    |           |
| Acoplanar jets:  | 3.71 / 6 | –      | –  | 30.4 / 21 |
| Acoplanar leptons:                                     | n.a.     | –      | –  | –         |
| Events in all channels                                 |          | –      | –  | 30.4 / 21 |
| Limit ( $\text{GeV}/c^2$ ) exp. (median) at 95% CL:    | 109.5    | 103.4  | –  | 103.8 (*) |
| Limit ( $\text{GeV}/c^2$ ) observed at 95% CL:         | 107.2    | 102.5  | –  | 105.8     |

Table 8: *Information related to the searches of the four LEP experiments for ‘invisible’ Higgs decays at energies between 200 and 209 GeV (year 2000 data). DELPHI and L3 did not contribute data from year 2000; the DELPHI limits are from the previous years’ data. As usual, the ALEPH confidence level estimator is different from that employed here. (\*) OPAL quotes the average instead of the median expected limit*

The value of the log-likelihood for the combined experiment is shown in Figure 21. There are noticeable deviations from the expectation, at the level of about two sigmas.

The consistency of the combined data with the background expectation can be seen in Figure 22. There is an extreme minimum of  $1 - CL_b$  of 0.018 at  $110.2\text{GeV}/c^2$ , as expected from the  $-2 * \ln(Q)$  curve. There is also a *maximum* of 0.986 at  $83\text{ GeV}/c^2$ , corresponding to a deficit of candidates. Each of these deviations is a little over two sigma, and not especially unusual.

The  $CL_s$  curve shown in Figure 23 gives the limit on  $M_H$  assuming a 100% branching ratio into invisible modes.

The excluded region in the  $M_H$  v  $Br(H \rightarrow X)$  plane is shown in Figure 24. For most masses the exclusion is somewhat stronger than expected, but this reverses above  $105\text{ GeV}/c^2$ . The combination has not been performed for masses below  $80\text{ GeV}/c^2$ .

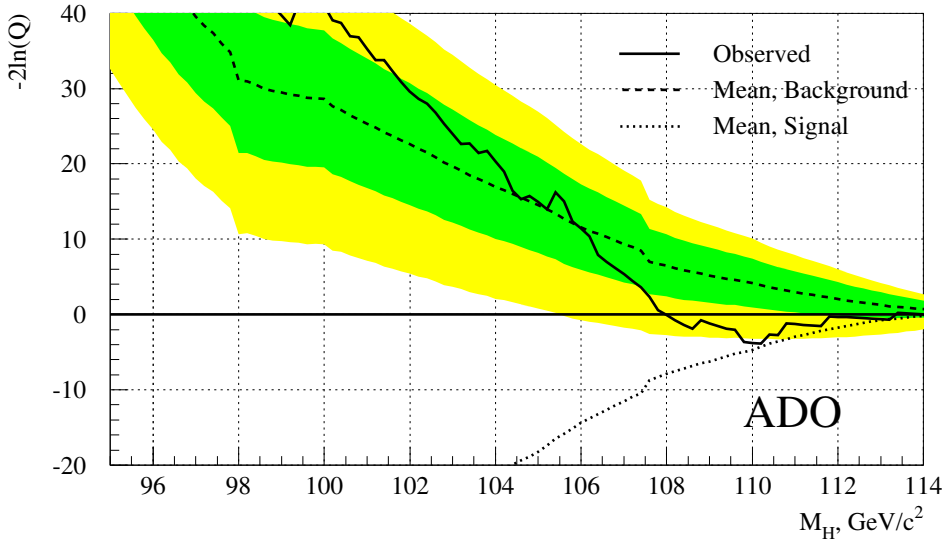


Figure 21: The distribution of  $-2\ln(Q)$  for the combined search for  $h^0 \rightarrow x$  by ALEPH, DELPHI and OPAL.

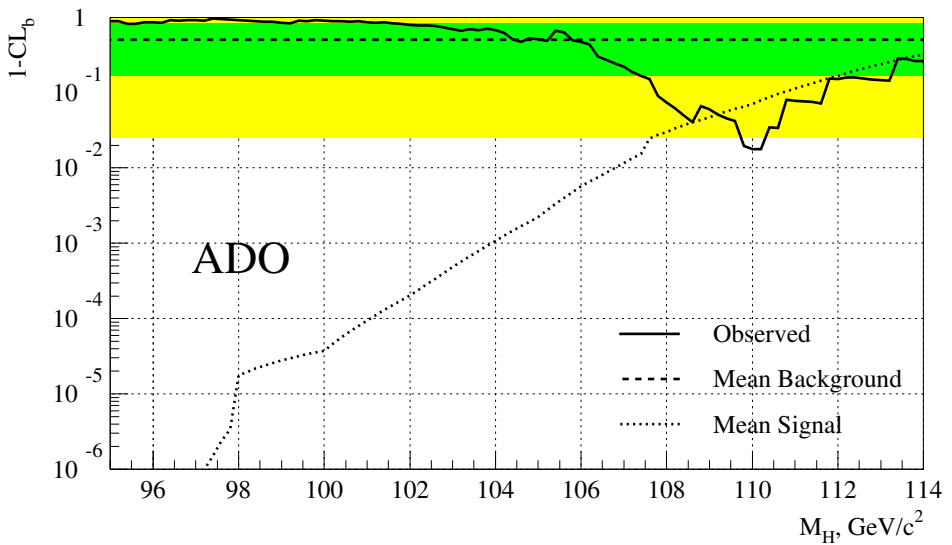


Figure 22: The value of  $1 - CL_b$  for the A,D,O combined data in the  $h^0 \rightarrow x$  search. The step nature of the result comes because ALEPH used a sliding window analysis, and report relevant candidates in a discretised way. There is a 'knee' in the curve of signal expectations; below 98  $\text{GeV}/c^2$  the ALEPH results from lower energies contribute.

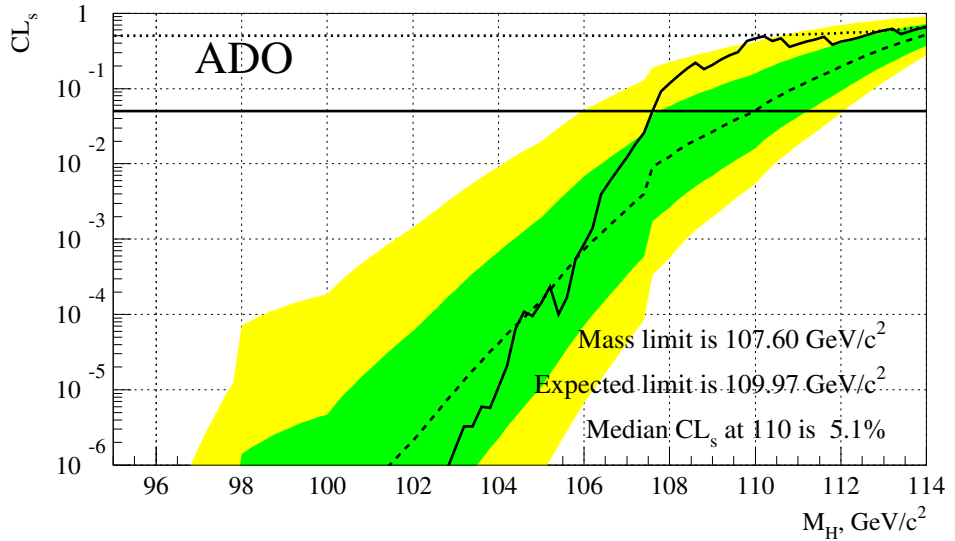


Figure 23: The value of  $CL_s$  for the  $A,D,O$  combined data in the  $h^0 \rightarrow \text{Invisible}$  search. The expected limit of  $110.0 \text{ GeV}/c^2$  for a 100% branching ratio into invisible modes is reduced to  $107.6$  by a small excess of candidates.

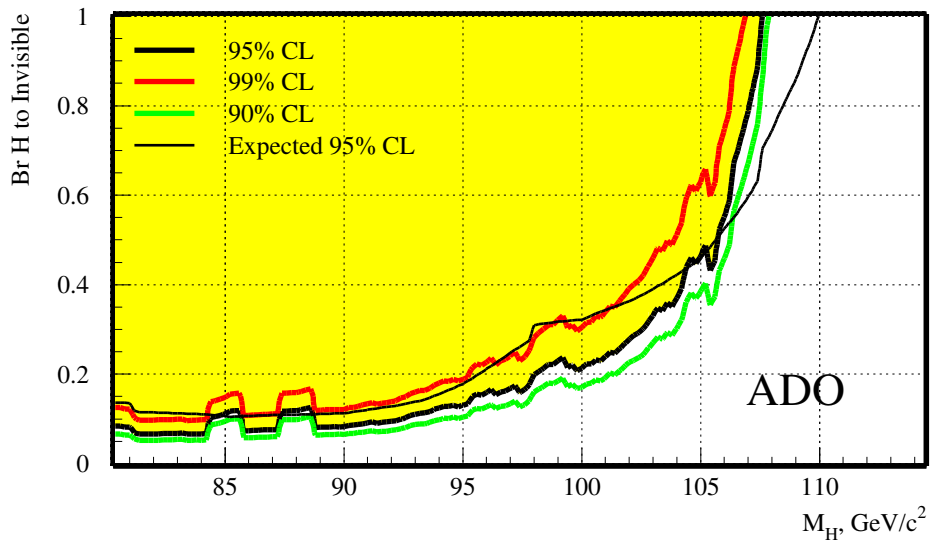


Figure 24: The region excluded by the  $A,D,O$  result in the  $h^0 \rightarrow \text{Invisible}$  search. The filled area corresponds to a 95% exclusion; 90 and 99% exclusion contours are shown for comparison, and the results are similar.

## 7 Summary

The LEP working group for Higgs boson searches has updated its previous combined limit for the mass of the Standard Model Higgs boson including the data collected in the year 2000 at energies between 200 and 209 GeV, for a total integrated luminosity of approximately  $350 \text{ pb}^{-1}$ . In the absence of a statistically significant excess in the data, a new lower bound of  $113.3 \text{ GeV}/c^2$  has been obtained at the 95% confidence level.

The working group has also searched for a possible signal for the  $h$  and  $A$  bosons in the MSSM scenario and produced new combined 95% confidence level limits for  $m_h$ ,  $m_A$  and  $\tan\beta$  for two representative MSSM scenarios. For  $\tan\beta > 0.4$  and the top quark mass less than or equal to  $174.3 \text{ GeV}/c^2$ , the limits  $m_h > 90.5 \text{ GeV}/c^2$  and  $m_A > 90.5 \text{ GeV}/c^2$  are obtained. Within the MSSM scenario which maximises the parameter space in the  $(m_h, \tan\beta)$  projection, values of  $\tan\beta$  between 0.5 and 2.3 are excluded at the 95% confidence level. This excluded range shrinks to 0.7-1.9 if the top mass is increased by its current experimental uncertainty of  $5.1 \text{ GeV}/c^2$ . Although the limits shown are representative for the bulk of possible MSSM parameter values, these should not be regarded as absolute exclusion limits. In a general scan where the parameters are allowed to vary independently, some rare combinations predict low production cross-sections or experimental signatures which make it difficult to separate the signal from the background.

The search results of the four LEP experiments for charged Higgs bosons predicted by models with two Higgs field doublets were also combined. These searches assume that the two decays  $H^+ \rightarrow c\bar{s}$  and  $H^+ \rightarrow \tau^+ \nu$  exhaust the  $H^+$  decay width. In the absence of a signal, mass limits are obtained as a function of the branching ratio  $B(H^+ \rightarrow \tau^+ \nu)$ . The most general lower limit, valid at the 95% confidence level for any value of the branching ratio, is  $77.4 \text{ GeV}/c^2$ .

The searches for Higgs boson photonic decays find the data to be consistent with Standard Model backgrounds throughout the range of sensitivity. For the “benchmark” fermiophobic Higgs boson, masses below  $106.4 \text{ GeV}$  are excluded by the four LEP experiments.

The search for ‘invisible’ decays of the Higgs boson has been performed and finds no statistically significant excess. We deduce a lower limit on the existence of a Higgs with the Standard Model production cross-section and 100% branching ratio into invisible modes of  $107.6 \text{ GeV}/c^2$ .

ALL THE RESULTS QUOTED IN THIS NOTE ARE PRELIMINARY.

## Appendix A: Combined confidence levels

In the SM and the MSSM, the signal and background rates are predicted channel by channel. The corresponding search results can thus be combined for a better overall sensitivity. Furthermore, datasets from different LEP energies and experiments can also be added. The combined LEP data are used to test two hypotheses: the *background-only* (“ $b$ ”) hypothesis, which assumes no Higgs boson to be present in the mass range investigated, and the *signal + background* (“ $s + b$ ”) hypothesis, where Higgs bosons are assumed to be produced according to the model under consideration. A global *test-statistic*  $X$  is constructed (see below) which allows the experimental result  $X_{\text{observed}}$  to be classified between the  $b$ -like and  $s + b$ -like situations. It utilises the number of selected events and various distributions which provide discrimination between signal and background (e.g., the reconstructed mass or b-tag variables). The test-statistic takes into account experimental details such as detection efficiencies, signal-to-background ratios, resolution functions, and provides a single value for a given model hypothesis (e.g., the test-mass  $m_H$  in the SM).

To set the scale for  $X$ , a large number of Monte Carlo experiments are generated, separately for the  $b$  and the  $s + b$  hypotheses, and separately for each model hypothesis (e.g.,  $m_H$ ). The resulting distributions of  $X(m_H)$  are normalised to become probability density functions, and integrated to form the confidence levels  $CL_b(m_H)$  and  $CL_{s+b}(m_H)$ . The integration starts in both cases from the  $b$ -like end and runs up to  $X_{\text{observed}}$ ; thus  $CL_b(m_H)$  and  $CL_{s+b}(m_H)$  express the probabilities that the outcome of an experiment is more  $b$ -like or less  $s + b$ -like, respectively, than the outcome represented by the set of selected events.

When performing a search with small expected signal rates, it may happen that the observed number of candidates is far below the expected background level. In such cases the limit may extend beyond the range of sensitivity of the search. To prevent *a priori* such unphysical, but formally valid, results from occurring, we consider the ratio  $CL_s(m_H) = CL_{s+b}(m_H)/CL_b(m_H)$  as a conservative approximation to the signal confidence one might have obtained in the absence of background. The 95% CL lower limit for the SM Higgs mass is defined here as the lowest value of the test mass  $m_H$  which yields  $CL_s(m_H) = 0.05$ .

The quantity  $1 - CL_b(m_H)$  is an indicator for a possible signal: a SM Higgs boson with true mass  $m_0$  would produce a pronounced drop in this quantity for  $m_H \approx m_0$ . Values of  $1 - CL_b < 5.7 \times 10^{-7}$  ( $1 - CL_b < 2.7 \times 10^{-3}$ ) would indicate a  $5\sigma$  ( $3\sigma$ ) discovery. Background fluctuations may also produce such a drop, allowing for some  $m_H$  a “discovery” beneath the expected experimental sensitivity. In analogy to the definition of  $CL_s$ , an additional quantity  $(1 - CL_b)' = (1 - CL_b)/(1 - CL_{s+b})$  is defined to incorporate information about signal sensitivity into the discovery estimator. This additional information is provided for informational purposes where appropriate.

If values of  $X_{\text{observed}}$  (and thus the integration bounds) are obtained from Monte Carlo simulations of the real experiment, the average expected confidence levels  $\langle 1 - CL_b(m_H) \rangle$  and  $\langle CL_s(m_H) \rangle$  are obtained. Of particular interest are  $\langle 1 - CL_b(m_H) \rangle$  from simulated  $s + b$  experiments and  $\langle CL_s(m_H) \rangle$  from simulated  $b$  experiments, since these indicate the expected ranges of sensitivity of the available data set for discovery and exclusion, respectively.

The test-statistic adopted in the present combination of results is the ratio of the likelihood function for the  $s+b$  hypothesis ( $x = s(m_H)$ ) to the likelihood function for the  $b$  hypothesis ( $x = 0$ ):

$$X(m_H) = \frac{\mathcal{L}(s(m_H))}{\mathcal{L}(0)}, \quad (1)$$

where the likelihood function is defined by

$$\mathcal{L}(x) = \prod_{i=1}^N \frac{\exp[-(x \frac{s_i(m_H)}{s(m_H)} + b_i)] (x \frac{s_i(m_H)}{s(m_H)} + b_i)^{n_i}}{n_i!} \times \prod_{j=1}^{n_i} \frac{x \frac{s_i(m_H)}{s(m_H)} S_i(m_H, m_{ij}) + b_i B_i(m_{ij})}{x \frac{s_i(m_H)}{s(m_H)} + b_i}. \quad (2)$$

The index  $i$  runs over all independent contributions to the combined search result: search channels of an experiment, searches at different centre-of mass energies, and channels from different experiments. The symbol  $N$  stands for the number of such contributions (“channels” hereafter);  $n_i$  is the number of observed candidates in channel  $i$  and  $m_{ij}$  is the value of  $m$ , (the reconstructed Higgs boson mass or any other discriminating variable) in the case of candidate  $j$  in channel  $i$ . The quantities  $s_i(m_H)$  and  $b_i$  are the integrated signal and background rates in channel  $i$  with  $s(m_H) = \sum_{i=1}^N s_i(m_H)$  and  $b = \sum_{i=1}^N b_i$  as the total expected signal and background in all channels. The functions  $S_i(m_H, m)$  and  $B_i(m)$  are the probability distributions for the signal and background, respectively. The above notation assumes that the background-related quantities  $b_i$  and  $B_i(m)$  do not depend on  $m_H$ . If the selection criteria in any one channel are  $m_H$  dependent,  $b_i$  and  $B_i(m)$  have to be replaced by  $b_i(m_H)$  and  $B_i(m_H, m)$ .

The above test-statistic makes the most efficient use of the information available in a search result in a manner similar to the way the principle of maximum likelihood gives the most efficient estimators of parameters in a measurement.

The calculation of confidence levels is illustrated in Figure 25. In part (a) the probability distributions of the test-statistic  $X$  (designated here by  $Q$ ) are shown for the  $s+b$  and the  $b$  hypotheses. In part (b) the confidence levels  $CL_b$ ,  $CL_{s+b}$  and  $CL_s$  are shown (the latter two are indistinguishable in the present example); they are obtained by integrating the probability distributions in (a) from right to left (from most to least background-like). The shaded areas in part (a) measure the confidence levels which correspond to the 95% confidence level exclusion limit.

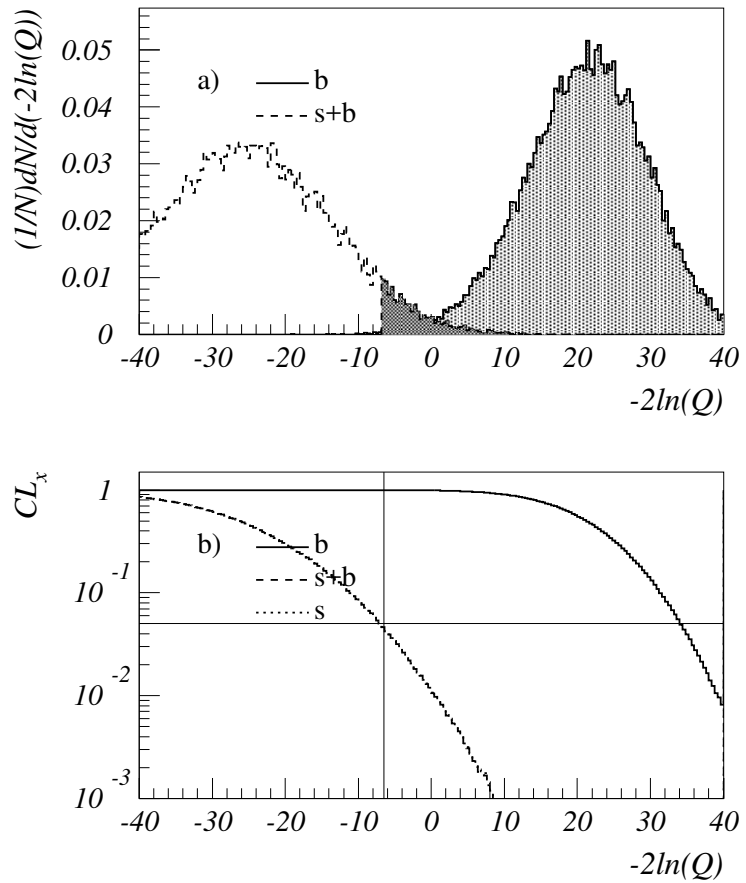


Figure 25: (a) An example of the probability distributions for the test statistic  $X$  (designated here by  $Q$ ) for background “ $b$ ” and signal “ $s+b$ ” gedanken experiments. The shaded areas indicate the integrals, from right (most “ $b$ ”-like) to left, up to the value indicated by the vertical line. This defines the confidences  $CL_b$ ,  $CL_{s+b}$  and  $CL_s = CL_{s+b}/CL_b$  (the latter two are indistinguishable in this example) which are shown in (b).

## Appendix B: MSSM benchmark scans

We present limits in the MSSM parameter space for a constrained MSSM with seven parameters,  $M_{\text{SUSY}}$ ,  $M_2$ ,  $\mu$ ,  $A$ ,  $\tan\beta$ ,  $m_A$  and  $m_{\tilde{g}}$ . Universal values  $M_{\text{SUSY}}$  and  $M_2$  are assumed for the SUSY breaking sfermion and gaugino masses, respectively, at the electroweak scale, and  $M_1$  is derived from  $M_2$  using the GUT relation  $M_1 = M_2(5 \sin^2 \theta_W / 3 \cos^2 \theta_W)$ , where  $\theta_W$  is the weak mixing angle. The gluino mass  $m_{\tilde{g}}$  is fixed in the scenarios described below in order to emphasise its effect via radiative corrections to  $m_h$ .  $\mu$  is the supersymmetric Higgs boson mass parameter, and  $\tan\beta$  is the ratio of the vacuum expectation values of the two Higgs field doublets. The parameter  $A$  is the common trilinear Higgs-squark coupling parameter, assumed to be the same for up-type squarks and for down-type squarks. The largest contributions to  $m_h$  from radiative corrections arise from top/stop loops, with much smaller contributions from bottom and sbottom loops.

In the scenarios that follow, it is not  $A$  which is specified, but rather the off-diagonal top mass coefficient in the stop mixing matrix [4]  $X_t = A - \mu \cot\beta$  which is set to a fixed value. The mass of the top quark is taken to be 174.3 GeV, but values smaller and larger by the current experimental error of 5.1 GeV are also considered in the  $\tan\beta$  exclusions, given in Table 4. The gluino mass  $m_{\tilde{g}}$  affects loop corrections from stops and sbottoms. Three benchmark scenarios are considered in this paper.

### The no-mixing scenario

This scenario assumes that there is no mixing in the scalar top sector, with the following values and ranges for the parameters:  $M_{\text{SUSY}} = 1$  TeV,  $M_2 = 200$  GeV,  $\mu = -200$  GeV,  $X_t = 0$ ,  $0.4 < \tan\beta < 50$  and  $m_A < 1$  TeV. The gluino mass  $m_{\tilde{g}}$  is set to 800 GeV.

### The $m_h$ -max scenario

This scenario is designed to maximise the largest value of  $m_h$  allowed at each value of  $\tan\beta$ . The same parameters are chosen as for the no-mixing scenario, except for the stop mixing parameter  $X_t = 2M_{\text{SUSY}}$  using the conventions of the two-loop diagrammatic calculation of [32] or  $X_t = \sqrt{6}M_{\text{SUSY}}$  using the conventions of the renormalisation-group approach of [33]. (For the no-mixing scenario,  $X_t = 0$  has the same interpretation in both schemes.) It is similar in spirit to the “maximal mixing” scenario used in previous publications [10], but as it allows for larger  $m_h$  values at the same  $\tan\beta$ , it results in more robust excluded intervals of  $\tan\beta$ .

### The $large - \mu$ scenario

This scenario is designed to highlight choices of MSSM parameters for which the Higgs boson  $h^0$  does not decay into pairs of b quarks due to large loop corrections. The parameters chosen are  $M_{\text{SUSY}} = 400$  GeV,  $\mu = 1$  TeV,  $M_2 = 400$  GeV,  $m_{\tilde{g}} = 200$  GeV,  $4 \leq m_A \leq 400$  GeV,  $X_t = -300$  GeV in both schemes described above. For the Feynman-diagrammatic calculation [32],  $m_b$  is set to 3 GeV in order to absorb higher-order QCD corrections, important for controlling the effects of large sbottom mixing at large  $\mu$  and  $\tan\beta$ . For the RGE-improved calculation, the dominant one-loop QCD and SUSY-QCD corrections are resummed to all orders [34]. An

important feature of this scenario is that  $m_h < 107.9 \text{ GeV}/c^2$  over the region of the  $(m_A, \tan \beta)$  plane under consideration. Only in regions where  $B(h^0 \rightarrow b\bar{b}) \approx 0$  are there potential weaknesses.

The HZHA program, version 3 [2], has been used to compute the Higgs boson masses, production cross-sections and decay branching ratios. For the *no-mixing* and  $m_h$ -*max* scenarios it has been modified to include the diagrammatic calculations of Ref. [32] while for the large- $\mu$  scenario the RGE-approach [33] has been used. For the *no-mixing* and  $m_h$ -*max* scenarios,  $\tan \beta$  is only investigated up to 30, due to the fact that the  $h$  decay width can exceed the detector resolution. Experimental results currently assume that the Higgs bosons have negligible width; Higgs bosons with decay widths equal to or larger than the experimental resolution can only be reconstructed with lower signal/background ratios, yielding weaker limits.

## References

- [1] ALEPH, DELPHI, L3 and OPAL Collab., The LEP working group for Higgs boson searches, *Searches for Higgs bosons: Preliminary combined results using LEP data collected at energies up to 202 GeV*, CERN-EP/2000-055.
- [2] HZHA: P. Janot, in CERN Report 96-01, Vol. 2, p. 309 (1996); Version 3, released in December 1999, <http://alephwww.cern.ch/janot/Generators.html>.
- [3] R.D. Cousins and V.L. Highland, Nucl. Instr. Methods **A320** (1992) 331.
- [4] M. Carena, S. Heinemeyer, C.E.M. Wagner and G. Weiglein, *Suggestions for Improved Benchmark Scenarios for Higgs-Boson Searches at LEP2*, CERN-TH/99-374, DESY 99-186, hep-ph/9912223.  
S. Heinemeyer, W. Hollik, G. Weiglein, JHEP 0006 (2000) 009.
- [5] ALEPH Collab., ALEPH 00-064 CONF 00-042 (2000) (Contributed paper 262 to ICHEP 2000).
- [6] ALEPH Collab., ALEPH 00-006 CONF 00-003 (2000).
- [7] DELPHI Collab., DELPHI 2000-077 CONF 376 (2000) (contributed paper 275 to ICHEP 2000). DELPHI Collab., DELPHI 2000-092 CONF 391 (2000) (contributed paper 619 to ICHEP 2000).
- [8] L3 Collab., L3 note 2588, (2000).
- [9] OPAL Collab., OPAL PN436 (2000).
- [10] ALEPH, DELPHI, L3 and OPAL Collab., The LEP working group for Higgs boson searches, CERN EP 98-046 (1998).
- [11] W.-M. Yao, *Standard Model Higgs and Top Mass Measurements at the Tevatron*, FERMILAB-CONF-99/100-E.

- [12] L3 Collab., L3 note 2573 (2000).
- [13] P. McNamara, Presentation to the LEP Experiments Committee, 7 September 1999. Available at <http://lephiggs.web.cern.ch/LEPHIGGS/talks/index.html>.
- [14] A. Djouadi, J. Kalinowski and P.M. Zerwas, Z. Phys. **C57** (1993) 569.
- [15] Charged Higgs inputs of the four experiments.  
 ALEPH Collab., ALEPH 2000-011 CONF 2000-008 (2000). See Reference [5] for the 2000 data update. DELPHI Collab., DELPHI 2000-077 CONF 376 (2000) (contributed paper 275 to ICHEP 2000) and DELPHI 2000-091 CONF 390 (2000) (contributed paper 613 to ICHEP 2000);  
 L3 Collab., L3 note 2549 (2000);  
 OPAL Collab. OPAL PN436 (2000).
- [16] A. Denner et al., Phys. Lett. **B475** (2000) 127;  
 M. Skrzypek et al., *Precision Calculation of Heavy Boson Production - YFS Monte Carlo Approach*, hep-ph/9903379.
- [17] J. Ellis, M.K. Gaillard, and D.V. Nanopoulos, Nucl. Phys. **B106** (1976) 292.
- [18] K. Hagiwara and M.L. Stong, Zeit. Phys. **C62** (1994) 99.
- [19] H. Haber, G. Kane and T. Sterling, Nucl. Phys. **B161** (1979) 493.
- [20] A.G. Akeroyd, Phys. Lett. **B368** (1996) 89; L. Brúcher, R. Santos, Eur. Phys. J. **C12** (2000) 87.
- [21] A. Stange, W. Marciano and S. Willenbrock, Phys. Rev. **D49** (1994) 1354.
- [22] J.F. Gunion, R. Vega and J. Wudka, Phys. Rev. **D42** (1990) 1673.
- [23] ALEPH Collab., ALEPH Conf. Abstract 260 (2000) (contributed paper to ICHEP 2000);  
 ALEPH Collab., R. Barate *et al.*, CERN-EP/2000-083 (2000), submitted to Phys. Lett. B.
- [24] DELPHI Collab., P. Abreu *et al.*, DELPHI 2000-082 (2000) (contributed paper to ICHEP 2000);  
 DELPHI Collab., P. Abreu *et al.*, Phys. Lett **B458** (1999) 431.
- [25] L3 Collab., L3 Note 2580 (2000), L3 Collab., L3 Note 2595 (2000), (contributed papers to ICHEP 2000).
- [26] OPAL Collab., OPAL PN450 (2000) (contributed paper to ICHEP 2000);  
 OPAL Collab., G. Abbiendi *et al.*, Phys. Lett. **B464** (1999) 311;  
 OPAL Collab., K. Ackerstaff *et al.*, Phys. Lett. **B437** (1998) 218;  
 OPAL Collab., K. Ackerstaff *et al.*, Eur. Phys. **C1** (1998) 31.

- [27] A. Djouadi, J. Kalinowski and M. Spira, Comp. Phys. Comm. **108** (1998) 56.
- [28] ALEPH Collab., ALEPH 2000-009, CONF 2000-006 (2000); // ALEPH Collab., CERN-EP/99-125 (1999).
- [29] DELPHI  $h^0 \rightarrow$  invisible DELPHI Collab., DELPHI 2000-078 CONF 377 (2000) (contributed paper 276 to ICHEP 2000);
- [30] OPAL Collab., OPAL PN436 (2000).
- [31] D. Bardin et al., Nucl. Phys. B, Proc. Suppl. **37B** (1994) 148; Comp. Phys. Comm. **104** (1997) 161;  
F.A. Berends et al., Comp. Phys. Comm. **85** (1995) 437; Nucl. Phys. **454** (1995) 437.
- [32] S. Heinemeyer, W. Hollik and G. Weiglein, Phys. Rev. **D58** (1998) 091701; Eur. Phys. Journ. **C9** (1999) 343.
- [33] M. Carena, M. Quirós and C.E.M. Wagner, Nucl. Phys. **B461** (1996) 407, hep-ph/9508343.
- [34] M. Carena, C.E.M. Wagner, S. Mrenna, CERN-TH/99-203, hep-ph/9907402 (1999).